Virology 404 (2010) 187–203

Contents lists available at ScienceDirect

Virology

journal homepage: www.elsevier.com/locate/yviro

Comparison of the replication and persistence of simian-human immunodeficiency viruses expressing Vif proteins with mutation of the SLQYLA or HCCH domains in macaques

Kimberly Schmitt [a], M. Sarah Hill [b], Zhenqian Liu [b], Autumn Ruiz [a], Nathan Culley [c], David M. Pinson [d], Edward B. Stephens [a,b,*]

[a] Department of Anatomy and Cell Biology, University of Kansas Medical Center, Kansas City, KS 66160, USA
[b] Department of Microbiology, Molecular Genetics and Immunology, University of Kansas Medical Center, Kansas City, KS 66160, USA
[c] Laboratory Animal Resources, University of Kansas Medical Center, Kansas City, KS 66160, USA
[d] Laboratory Medicine and Pathology, University of Kansas Medical Center, Kansas City, KS 66160, USA

ARTICLE INFO

Article history:
Received 20 January 2010
Returned to author for revision
17 February 2010
Accepted 18 April 2010
Available online 3 June 2010

Keywords:
Vif
Simian-human immunodeficiency virus
SHIV
Rhesus macaques
APOBEC3G
APOBEC3F
Replication
BC box
Zn binding motif

ABSTRACT

The Vif protein of primate lentiviruses interacts with APOBEC3 proteins, which results in shunting of the APOBEC3-Vif complex to the proteosome for degradation. Using the simian-human immunodeficiency virus (SHIV)/macaque model, we compared the replication and pathogenicity of SHIVs that express a Vif protein in which the entire SLQYLA ($SHIV_{Vif5A}$) or HCCH ($SHIV_{VifHCCH(-)}$) domains were substituted with alanine residues. Each virus was inoculated into three macaques and various viral and immunological parameters followed for 6 months. All macaques maintained stable circulating $CD4^+$ T cells, developed low viral loads, maintained the engineered mutations, yielded no histological lesions, and developed immunoprecipitating antibodies early post-inoculation. Sequence analysis of *nef* and *vpu* from three lymphoid tissues revealed a high percentage of G-to-A-substitutions. Our results show that while the presence of HCCH and SLQYLA domains are critical *in vivo*, there may exist APOBEC3 negative reservoirs that allow for low levels of viral replication and persistence but not disease.

Introduction

Human immunodeficiency virus type 1 (HIV-1) and other lentiviruses encode for a Vif (virion infectivity factor) protein, which has been shown to be essential for HIV-1 replication in primary $CD4^+$ T cells and macrophages (Fan and Peden, 1992; Gabuzda et al., 1992; Blanc et al., 1993; Sakai et al., 1993; von Schwedler et al., 1993; Borman et al., 1995). The Vif protein interacts with apolipoprotein B mRNA editing enzyme catalytic peptide-like 3G (APOBEC3G; hA3G) promoting its accelerated degradation by the proteosome (Sheehy et al., 2003). APOBEC3G is a cytidine deaminase that, if packaged into HIV-1Δ*vif* virions, induces cytidine deamination of newly synthesized minus-strand viral DNA from cytosines to uracils, leading to G to A transitions in plus strand synthesis (Jarmuz et al., 2002; Harris et al., 2003; Mariani et al., 2003; Mangeat et al., 2003; Sheehy et al., 2003; Yu et al., 2004a). The RNA editing activity of the APOBEC3 family of proteins involves an active site characterized by a conserved zinc-binding motif, (Cys/His)-Xaa-Glu-Xaa_{23-28}-Pro-Cys-Xaa_{2-4}-Cys, containing a glutamate involved in proton shuttling during deamination (Jarmuz et al., 2002). In addition to A3G, humans have six other APOBEC3 genes; hA3A, hA3B, hA3C, hA3DE, hA3F, and hA3H (Jarmuz et al., 2002). Of those APOBEC3 genes, hA3B, hA3DE, hA3G, and hA3F, have been shown to inhibit the replication of HIV-1Δ*vif* (Dang et al., 2006, 2008; Doehle et al., 2005; Wiegand et al., 2004; Yang et al., 2007; Yu et al., 2004b; Zheng et al., 2004). SIV_{mac}239Δ*vif* has been shown to be restricted by hA3G, hA3F, hA3B, hA3C, hA3DE (Dang et al., 2006, 2008; Mariani et al., 2003; Yu et al., 2004b; Zennou and Bieniasz, 2006). The HIV-1 Vif has limited activity against rhesus and African green monkey A3 proteins while Vif from SIV_{mac}239 and SIV_{agm} have broader specificities. While less is presently known about the rhesus A3 proteins, it is known that HIV-1Δ*vif* can be inhibited by rhA3G, rhA3F, rhA3B, and to a lesser extent rhA3H and rhA3DE (Virgen and Hatziioannou, 2007). SIV_{mac}239Δ*vif* has been shown to be restricted by rhA3G, rhA3F, rhA3C, rhA3B and rhA3DE, and to a lesser extent rhA3H (Virgen and Hatziioannou, 2007; Zennou and Bieniasz, 2006).

* Corresponding author. Department of Microbiology, Molecular Genetics and Immunology, University of Kansas Medical Center, Kansas City, KS 66160, USA. Fax: +1 913 588 2710.
E-mail address: estephen@kumc.edu (E.B. Stephens).

0042-6822/$ – see front matter © 2010 Elsevier Inc. All rights reserved.
doi:10.1016/j.virol.2010.04.017

Sequence analysis of Vif proteins from different lentiviruses reveals that there are two highly conserved domains in the carboxyl terminus, the SLQ(Y/F)LA and Zn^{++} binding (HCCH) motifs. Previous cell culture studies with hA3 proteins showed that introduction of amino acid substitutions in the viral BC box (SLQ(Y/F)LA) resulted in decreased binding of Vif to Elongin C while substitutions in the HCCH domain prevent interactions with Cullin 5 of the Cul5/Elongin B/C/Rbx E3 ligase complex (Luo et al., 2005; Mehle et al., 2004a,b, 2006; Stopak et al., 2003; Yu et al., 2003, 2004c). These studies showed increased A3G incorporation into virions and G-to-A hypermutation (Mangeat et al., 2003; Shindo et al., 2003; Zhang et al., 2003). Our laboratory has been using the chimeric simian-human immunodeficiency (SHIV)/macaque model to study the role of Vpu and its various domains in $CD4^+$ T cell loss, virus release and pathogenesis (Stephens *et al.*, 2002; Singh *et al.*, 2003; Hout *et al.*, 2005; 2006; Hill et al., 2008). In this study, we constructed simian-human immunodeficiency viruses (SHIVs) in which five amino acids in the SLQYLA motif ($SHIV_{Vif5A}$) and four amino acids of the HCCH ($SHIV_{VifHCCH(-)}$) domain were changed to alanine residues. Our results indicate that rhA3F is stable in the presence of wild type and mutant Vif viruses and that rhA3G is more effective at cytidine deamination than rhA3F. Our results show that both the HCCH and SLQYLA domains were critical to Vif function *in vivo* but that production of viral RNA only persisted in macaques inoculated with the $SHIV_{VifHCCH(-)}$.

Results

Replication of $SHIV_{Vif5A}$ and $SHIV_{VifHCCH(-)}$ in APOBEC3 positive and negative cell lines

The sequence of the Vif mutants that were analyzed in this study are shown in Fig. 1. We performed assays to examine the replication of parental $SHIV_{KU\text{-}2MC4}$, $SHIV_{Vif5A}$, $SHIV_{VifHCCH(-)}$, $SHIV_{VifAAQYLA}$ and $SHIV_{VifSTOP}$ in hA3G/F positive (C8166) and negative (SupT1) cell lines as well as rhesus PBMC (rhA3G/F+). We included $SHIV_{VifAAQYLA}$ in these growth curves for comparison as we previously reported on the replication of this mutant in tissue culture and in macaques (Schmitt et al., 2009). Cells were inoculated with equivalent amounts (25 ng of p27) each of the virus and the levels of p27 Gag released into the culture medium were quantified using a commercial antigen capture assay. All four mutant viruses ($SHIV_{Vif5A}$, $SHIV_{VifHCCH(-)}$, $SHIV_{VifAAQYLA}$ and $SHIV_{VifSTOP}$) replicated in SupT1 cells to similar levels as parental $SHIV_{KU\text{-}2MC4}$ by day 15 post-inoculation, although the kinetics of replication were slower (Fig. 2A). Inoculation of equivalent amounts (25 ng p27) of $SHIV_{Vif5A}$, $SHIV_{VifHCCH(-)}$, $SHIV_{VifAAQYLA}$, and $SHIV_{VifSTOP}$ into hA3G/F+C8166 cell cultures resulted in less than 0.01% of the p27 released compared to parental $SHIV_{KU\text{-}2MC4}$ (Fig. 2B). As shown in Fig. 2C, in rhesus PBMC $SHIV_{KU\text{-}2MC4}$ replicated to high levels (7.932 ng/ml) while $SHIV_{VifHCCH(-)}$ (0.119 ng/ml) and $SHIV_{Vif5A}$ (0.197 ng/ml), and $SHIV_{VifAAQYLA}$ (0.11 ng/ml) replicated to low but detectable levels. Replication was undetectable for $SHIV_{VifSTOP}$ in rhesus PBMC.

Both $SHIV_{Vif5A}$ and $SHIV_{VifHCCH(-)}$ incorporate rhA3G and rhA3F into virus particles

The above results suggested that hA3G and hA3F or rhA3G and rhA3F might be incorporated into maturing virus particles resulting in restriction of replication. As we are most interested in rhA3G and rhA3F, we transfected 293 cells with plasmids expressing an HA-tagged rhA3G or a V5-tagged rhA3F and the complete genomes of either $SHIV_{Vif5A}$, $SHIV_{VifHCCH(-)}$, $SHIV_{VifSTOP}$, or parental $SHIV_{KU\text{-}2MC4}$. At 48 h post-transfection, the culture medium was collected, clarified, and the virus partially purified and concentrated by ultracentrifugation. Equal amounts of p27 (as determined by Western blot) were loaded and analyzed for the presence or absence of rhA3G or rhA3F. The results shown in Fig. 3A indicate that rhA3G was incorporated into $SHIV_{Vif5A}$, $SHIV_{VifHCCH(-)}$, and $SHIV_{VifSTOP}$ virus particles but was excluded from $SHIV_{KU\text{-}2MC4}$ particles. However, we found that the rhA3F protein was incorporated into all four viruses (Fig. 3B). These results indicate that rhA3G was selectively incorporated only into the Vif mutants while rhA3F was incorporated into all viruses. The inability of $SIV_{mac}239$ Vif to degrade and prevent the incorporation of rhA3F has been previously reported (Virgen and Hatziioannou, 2007).

Rhesus A3F is stable in the presence of $SIV_{mac}239$ Vif

Since we observed that rhA3F was incorporated into virus particles, we determined the stability of rhA3F and rhA3G in the presence of the viral genome. 293 cells were co-transfected with vectors expressing rhA3G or rhA3F and the genomes of $SHIV_{KU\text{-}2MC4}$, $SHIV_{Vif5A}$, $SHIV_{VifHCCH(-)}$, or $SHIV_{VifSTOP}$. Our results indicate that in the presence of the $SHIV_{KU\text{-}2MC4}$ genome, rhA3G was not stable whereas it was detected in the presence of the $SHIV_{Vif5A}$, $SHIV_{VifHCCH(-)}$ or $SHIV_{VifSTOP}$ (Fig. 4). We also found that rhA3F appeared to be stable in the presence of both $SHIV_{KU\text{-}2MC4}$ and also $SHIV_{Vif5A}$, $SHIV_{VifHCCH(-)}$, or $SHIV_{VifSTOP}$ genomes. However, it should be noted that we consistently found higher levels of rhA3F in the presence of the $SHIV_{VifSTOP}$ genome, indicating fundamental differences between the targeting site-directed Vif mutants and the absence of the Vif protein. The results obtained with rhA3F correlate well with the above experiment showing that rhA3F was incorporated into virus particles.

Rhesus A3G but not rhA3F causes significant G-to-A mutations in the nef gene of the SHIV genome

The results above indicated that significant levels of rhA3F were incorporated into virions and rhA3F was stable in cells expressing the wild type genome. We compared the level of G-to-A mutations of the SHIV genomes in the presence of either rhA3G or rhA3F. The results are shown in Fig. 5 and Table 1. Using viral genomes to express the Vif protein, we observed minimal G-to-A changes in $SHIV_{KU\text{-}2MC4}$ *nef* in the presence of either rhA3G or rhA3F. In the presence of rhA3G, we found that $SHIV_{Vif5A}$, $SHIV_{VifHCCH(-)}$ or $SHIV_{VifSTOP}$ *nef* had an increase in the number of G-to-A changes (from 2 to 24–29) or approximately 0.5% of the bases sequenced (Table 1). However, in the presence of

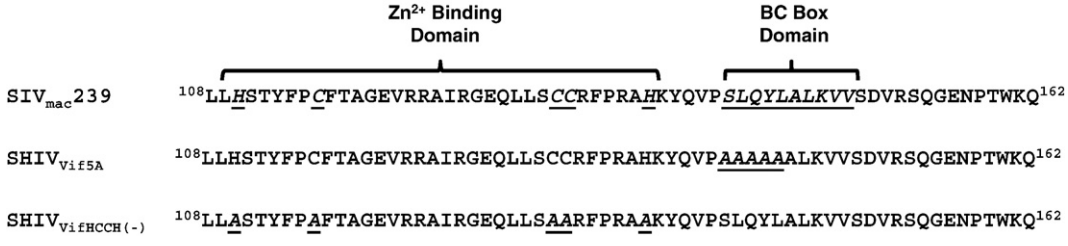

Fig. 1. Sequence of the wild type $SIV_{mac}239$ Vif protein and the two mutants analyzed in this study. The amino acids comprising the Zn^{+2} and BC box domains are italicized and underlined. The amino acid substitutions in the $SHIV_{Vif5A}$ and $SHIV_{VifHCCH(-)}$ are also underlined.

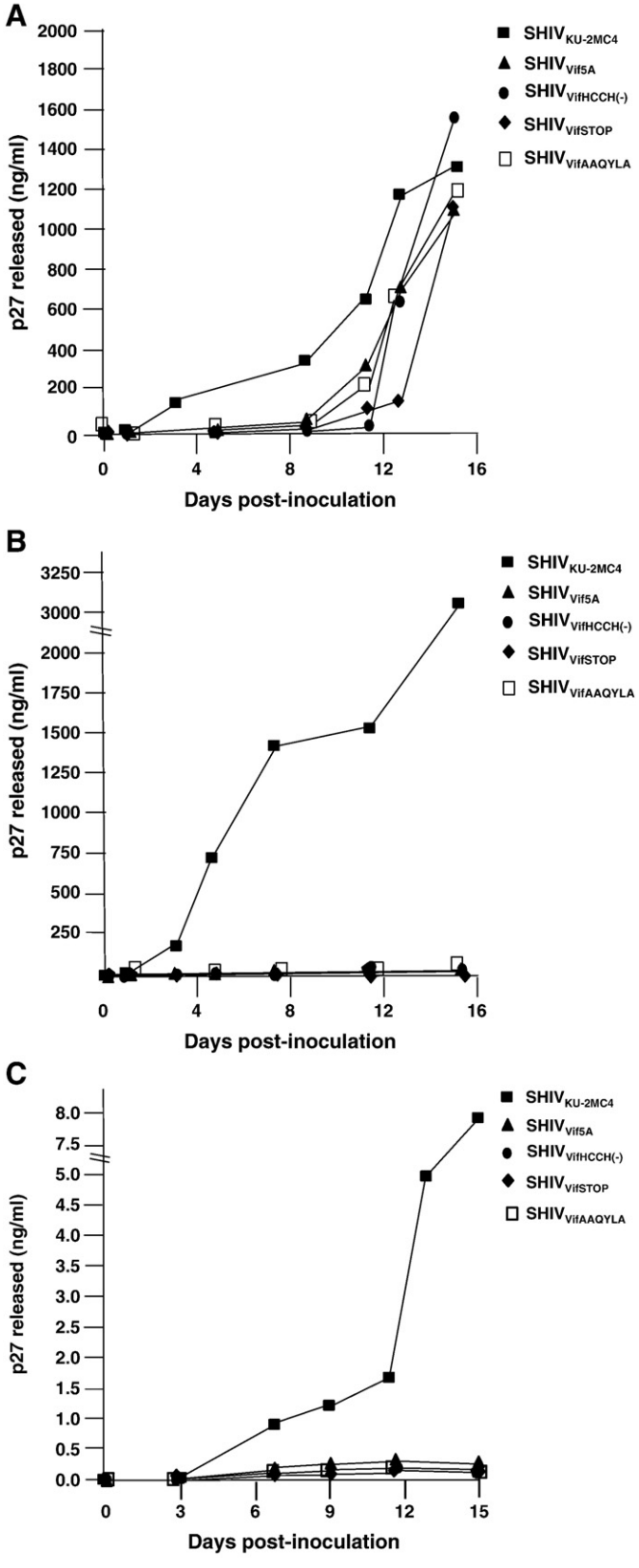

Fig. 2. Replication of $SHIV_{Vif5A}$, $SHIV_{VifHCCH(-)}$, $SHIV_{VifAAQYLA}$, $SHIV_{VifSTOP}$, and $SHIV_{KU-2MC4}$ in SupT1 cells (hA3G/F negative), C8166 cells (hA3G/F positive), and rhesus macaque PBMC. Cells were inoculated with equal amounts of each virus (25 ng of p27) and the levels of p27 in the culture supernatants were assessed at various times post-inoculation. Panel A. Replication of viruses in SupT1 cells. Panel B. Replication of viruses in C8166 cells. Panel C. Replication of viruses in rhesus PBMC. (▲) $SHIV_{Vif5A}$, (□) $SHIV_{VifAAQYLA}$(●) $SHIV_{VifHCCH(-)}$, (♦) $SHIV_{VifSTOP}$ and (■)$SHIV_{KU-2MC4}$.

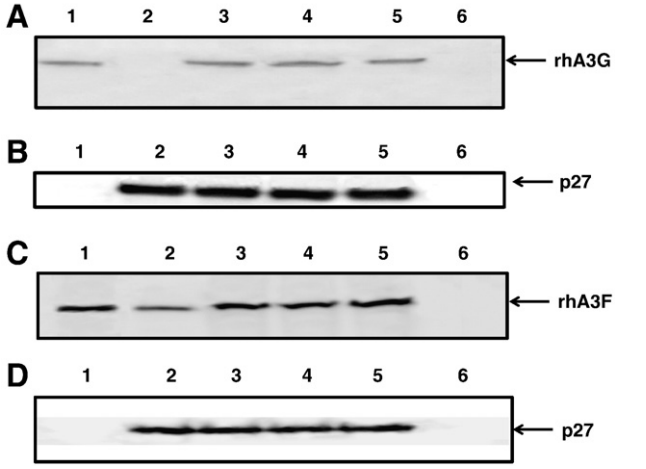

Fig. 3. The incorporation of rhA3G and rhA3F into virus particles. 293 cells were transfected with a plasmid that expressed the genome of either $SHIV_{KU-2MC4}$, $SHIV_{Vif5A}$, $SHIV_{VifHCCH(-)}$, or $SHIV_{VifSTOP}$ and a vector expressing HA-rhA3G or V5-rhA3F. At 48 h, the culture medium was collected, clarified by low speed centrifugation, and concentrated by ultracentrifugation through a 20/60 (w/v) step-gradient. Equivalent levels of p27 (determined by Western blot) from each sample were resuspended in sample reducing buffer, boiled, and the proteins were separated by SDS-PAGE. The presence of either rhA3G or rhA3F was detected by Western blot using an antibody directed against the HA-tag or V5 tag, respectively. Panel A. Results of rhA3G incorporation. Lane 1. rhA3G proteins detected in a lysate from cells transfected with vector expressing rhA3G alone. Lanes 2–5. rhA3G proteins detected in virus from cells transfected with vector expressing rhA3G and $SHIV_{KU-2MC4}$ (Lane 2), $SHIV_{Vif5A}$ (Lane 3), and $SHIV_{VifHCCH(-)}$ (Lane 4); and $SHIV_{VifSTOP}$ (Lane 5). In Lane 6, rhA3G proteins in the pelleted supernatant from cells transfected with empty vectors. Panel B. Blot in Panel A stripped and reprobed with an antibody against p27 protein. Panel C. Results of incorporation of rhA3F. Lane 1. rhA3F proteins detected in a lysate from cells transfected with vector expressing rhA3F alone. Lanes 2–5. rhA3F proteins detected in virus from cells transfected with vector expressing rhA3F and $SHIV_{KU-2MC4}$ (Lane 2), $SHIV_{Vif5A}$ (Lane 3), and $SHIV_{VifHCCH(-)}$ (Lane 4); and $SHIV_{VifSTOP}$ (Lane 5). In Lane 6, rhA3F proteins in the pelleted supernatant from cells transfected with empty vectors. Panel D. Blot in Panel C stripped and reprobed with an antibody against p27 protein.

rhA3F, we observed that $SHIV_{Vif5A}$, $SHIV_{VifHCCH(-)}$, and $SHIV_{VifSTOP}$ *nef* had a similar level of G-to-A changes compared to $SHIV_{KU-2MC4}$ (Table 1). The results with rhA3F suggest that incorporation of rhA3F does not result in significant G-to-A substitutions in *nef*.

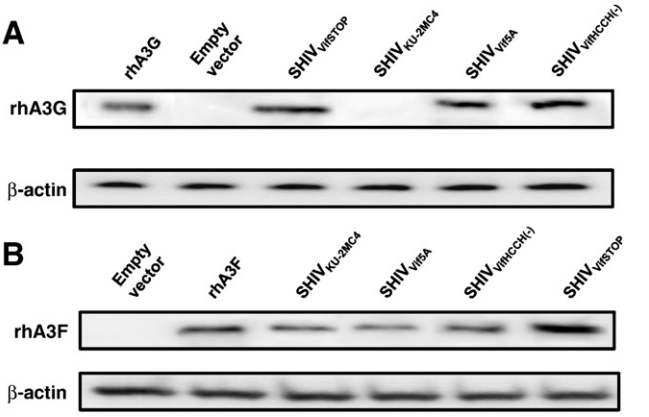

Fig. 4. Stability of the rhA3G and rhA3F in the presence of wild type and Vif mutant viral genomes. Full-length mutated SHIVs were co-transfected into 293 cells with a vector expressing either HA-rhA3G or V5-rhA3F. At 24 h post-transfection, cells were lysed and proteins were precipitated using methanol. Proteins were separated on a 10% SDS-PAGE gel and probed using an antibody directed against either the HA or V5-tag. All samples were normalized to the amount of β-actin protein. Panel A. Stability of rhA3G in the presence of $SHIV_{VifSTOP}$ (lane 3), $SHIV_{KU-2MC4}$ (lane 4), $SHIV_{Vif5A}$ (Lane 5), or $SHIV_{VifHCCH(-)}$ (Lane 6). Lanes 1 and 2 were used as a positive (rhA3G only; Lane 1) or negative (pcDNA3.1(+) only; Lane 2) control. Panel B. Stability of rhA3F in the presence of $SHIV_{KU-2MC4}$ (Lane 3), $SHIV_{Vif5A}$ (Lane 4), $SHIV_{VifHCCH(-)}$ (Lane 5), or $SHIV_{VifSTOP}$ (Lane 6). Lanes 1 and 2 were used as a negative (pcDNA3.1(+) only; Lane 1) or positive (rhA3F only; Lane 2) control.

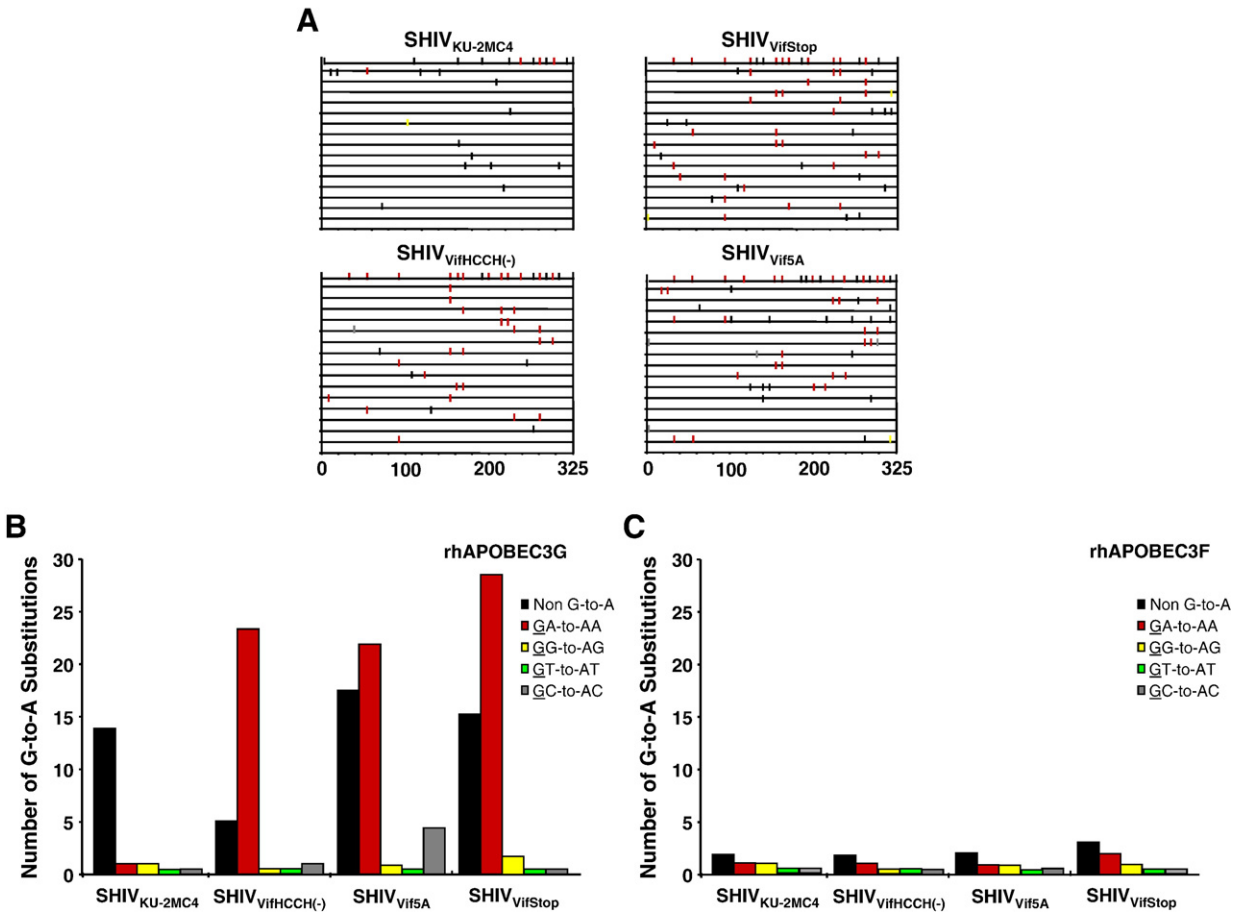

Fig. 5. Rhesus A3G but not rhA3F induces G-to-A mutations in single colony sequences obtained from *nef*. Full-length genomes of the wild type and Vif mutant viruses were co-transfected with vectors expressing either rhA3G or rhA3F into 293 cells. At 48 h post-transfection, the culture medium was collected, clarified by low speed centrifugation and used to infect TZM-bl cells. A 325 base pair fragment of *nef* was amplified from DNA at 24 h post-infection and assessed for G-to-A substitutions. Panel A. G-to-A mutations obtained from bulk (top line) and 15 independent clone sequences are shown. Each mutation is denoted by a vertical line that is color coded with respect to the dinucleotide context: non-G-to-A (black), GA to GA (red), GG to AA (yellow), GT to AT (cyan), or GC to AC (gray). Panels B and C. Graphs depicting the cumulative number of mutations from the 15 clones per virus in the presence of rhA3G and rhA3F, respectively. Post-transfection Panel C. Each bar is shaded according to the proportion of G-to-A-substitutions that occurred in the context of non-G-to-A (black). GA to AA (red), GG to AG (yellow), GT to AT (Cyan), GC to AC (gray).

Incorporation of rhA3G into virions results in restriction of virus replication

We examined the growth of $SHIV_{Vif5A}$, $SHIV_{VifSTOP}$, and $SHIV_{VifHCCH(-)}$ in the presence rhA3G or rhA3F restricted the production of infectious virus. 293 cells were transfected with the genomes of $SHIV_{Vif5A}$, $SHIV_{VifHCCH(-)}$, $SHIV_{VifSTOP}$, or $SHIV_{KU-2MC4}$ and a plasmid expressing either an HA-tagged rhA3G, V5-tagged rhA3F or the empty vector. At 48 h, the virus containing supernatant was collected, clarified by centrifugation, and the p27 levels quantified. Equivalent levels of p27 from each virus stock were used to titrate infectious virus by a series of 10-fold dilutions onto TZM.bl cells. At 48 h, the cells were stained for β-galactosidase activity (β-galactosidase is under the control of the LTR and expression of Tat from the incoming virus) and the number of $TCID_{50}$ determined. If rhA3G or rhA3F was packaged into the virions, the virus should be hypermutated resulting in the expression of a non-functional Tat. As shown in Fig. 6A, $SHIV_{KU-2MC4}$ replicated to approximately the same levels in the presence or absence (empty vector) of rhA3G while

Table 1
Results of the hypermutation assay of *nef* amplified by rhA3G and rhA3F in the presence of wild type and mutant Vif proteins.

APOBEC3 protein	Virus	[a]Total number of bases sequenced	Total # of G-to-A mutations/percent G-to-A mutations of bases sequenced	Number and context of cytidine deamination		
				5'-GA	5'-GG	5'-GC
rhA3G	$SHIV_{KU-2MC4}$	4875	2 (0.04)	1	1	0
rhA3G	$SHIV_{Vif5A}$	4875	24 (0.49)	23	0	1
rhA3G	$SHIV_{VifHCCH(-)}$	4875	26 (0.53)	21	1	4
rhA3G	$SHIV_{VifSTOP}$	4875	29 (0.59)	27	2	0
rhA3F	$SHIV_{KU-2MC4}$	4875	2 (0.04)	1	1	0
rhA3F	$SHIV_{Vif5A}$	4875	1 (0.02)	1	0	0
rhA3F	$SHIV_{VifHCCH(-)}$	4875	2 (0.04)	1	1	0
rhA3F	$SHIV_{VifSTOP}$	4875	3 (0.06)	2	1	0

[a] A 325 base fragment corresponding to the 5' end of *nef* was amplified, cloned and 15 individual clones were selected for sequence analysis.

the titers of $SHIV_{VifHCCH(-)}$, $SHIV_{Vif5A}$ and $SHIV_{VifSTOP}$ were 100- to 1000-fold less than the unmodified virus ($SHIV_{KU\text{-}2MC4}$). With rhA3F, our results indicate that $SHIV_{KU\text{-}2MC4}$, $SHIV_{VifHCCH(-)}$ and $SHIV_{Vif5A}$ had an approximate 10-fold decrease in titers and $SHIV_{VifSTOP}$ had greater than a 1000-fold decrease in titer (Fig. 6B). The results with rhA3F also emphasize the differences in site-directed mutations in $SHIV_{VifHCCH(-)}$, $SHIV_{Vif5A}$ and the severely truncated Vif in $SHIV_{VifSTOP}$.

Assessment of $SHIV_{VifHCCH(-)}$ replication in macaques

We inoculated three macaques with 10^4 $TCID_{50}$ of $SHIV_{VifHCCH(-)}$. Prior to inoculation, macaques AS34, AS51, and AV18 had circulating $CD4^+$ cell levels of 1,509, 1,109, and 400 cells per μl, respectively. These three macaques maintained levels of circulating $CD4^+$ T cells at pre-inoculation levels or higher throughout the course of the 6-month infection (Fig. 7A). All three macaques were euthanized at 26–28 weeks post-inoculation in excellent condition. At necropsy, AS34, AS51, and AV18 had circulating $CD4^+$ T cell levels of 2,124, 1,338, and 1,298 cells/μl, respectively. This contrasts with macaques inoculated with parental $SHIV_{KU\text{-}2MC4}$, which developed a severe loss of circulating $CD4^+$ T cells within 3–4 weeks post-inoculation (Fig. 7C). Analysis of the plasma viral loads revealed a mean viral load of 4.15×10^3 copies per ml at 1 week post-inoculation (Fig. 8A), which is approximately 10,000-fold less than the macaques inoculated with parental $SHIV_{KU\text{-}2MC4}$ (Fig. 8C). Following the first week of infection, the plasma viral loads in macaques AS34, AS51, and AV18 were at or just above the limits of detection. At necropsy, viral loads in all three macaques were undetectable. These results indicate that $SHIV_{VifHCCH(-)}$ transiently replicated in these macaques prior to control of the infection.

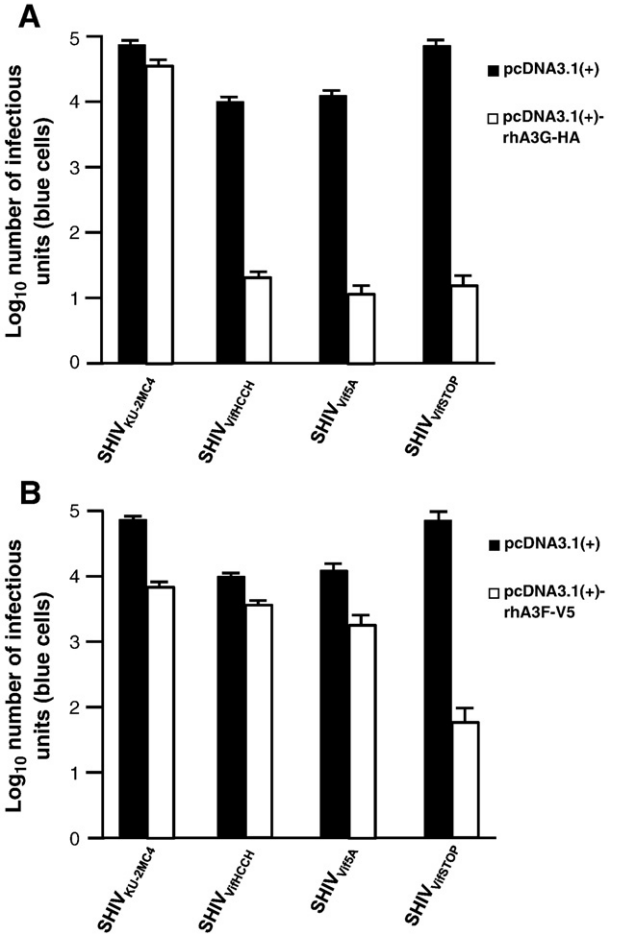

Fig. 6. Incorporation of rhA3G results in less infectious virus. 293 cells were co-transfected with the $SHIV_{KU\text{-}2MC4}$, $SHIV_{Vif5A}$, and $SHIV_{VifHCCH(-)}$ and $SHIV_{VifSTOP}$ genomes and plasmids expressing either rhA3G or rhA3F. Controls included co-transfection of each viral genome with empty plasmids (pcDNA3.1(+)). At 48 h, the culture medium was harvested, assessed for p27, and the amount of infectious virus titrated on the TZM.bl cells as described in Materials and methods. Shown are infectious titers in the absence or presence of either rhA3G (Panel A) or rhA3F (Panel B).

Assessment of $SHIV_{Vif5A}$ replication in macaques

We also assessed the ability of $SHIV_{Vif5A}$ to replicate in three macaques (CX54, ER65, and I92). Prior to inoculation, macaques CX54, ER65, and I92 had circulating $CD4^+$ T cell levels of 777, 844, and 1,451 cells per μl, respectively (Fig. 7B). These macaques, similar to those inoculated with $SHIV_{VifHCCH(-)}$, maintained circulating $CD4^+$ T cell levels near the pre-inoculation levels throughout the course of the 6-month infection. All three macaques were euthanized at 26 weeks post-inoculation in excellent condition. At necropsy, CX54, ER65, and I92 had circulating $CD4^+$ T cell levels of 513, 853, and 1192 cells per μl, respectively (Fig. 7B). This also contrasts with macaques inoculated with parental $SHIV_{KU\text{-}2MC4}$ (Fig. 7C). Analysis of the plasma viral loads of the macaques inoculated with $SHIV_{Vif5A}$ revealed a mean viral load of 1.3×10^3 copies per ml at 1 week post-inoculation (Fig. 8B). Following the first week of infection, the plasma viral loads in macaques CX54, ER65, and I92 fell to undetectable levels.

Mutations in vif amplified from isolated DNA of PBMC during the course of infection

We assessed the stability of the engineered mutations in the *vif* gene from DNA isolated PBMC throughout the course of infection. The *vif* sequence was amplified, directly sequenced and compared to the input *vif* sequence of $SHIV_{Vif5A}$ or $SHIV_{VifHCCH(-)}$. We observed that the engineered mutations were stable throughout the course of the 6-month infection for macaques inoculated with $SHIV_{VifHCCH(-)}$. We performed bulk sequencing of the *vif* amplified at 1, 2, 3, 4, 6, and 16 weeks. As shown in Fig. 9, the number of G-to-A mutations in the amplified *vif* gene increased with time in two (AS51, AV18) of the three macaques while the third macaque (AS34) appeared to have the largest number of G-to-A mutations at 3 weeks post-inoculation. As we had reported earlier, the majority of the G-to-A mutations were in the context of the 5'-T**C** (minus strand) rather than 5'-C**C** (Schmitt et al., 2009). We were able to amplify part of the *vif* sequence at 1 week from PBMC DNA isolated from macaques inoculated with $SHIV_{Vif5A}$ (CX54,ER65, I92). The sequence analysis also revealed that these *vif* mutations were stable at 1 week post-inoculation (data not shown). However, from 3 weeks until necropsy, we were unable to amplify the *vif* gene, which correlates with the undetectable plasma viral loads in these macaques after week 1 post-inoculation.

Macaques inoculated with $SHIV_{Vif5A}$ and $SHIV_{VifHCCH(-)}$ developed anti-viral antibody responses early after inoculation

We analyzed the plasma from infected macaques at 12 weeks and at necropsy (26–28 weeks) for the presence of immunoprecipitating antibody responses. At 12 weeks post-inoculation, all three macaques inoculated with $SHIV_{Vif5A}$ had developed antibody responses to p27 but only macaque ER65 developed antibody responses to the Env glycoprotein (Fig. 10A). For macaques inoculated with $SHIV_{VifHCCH(-)}$, all three macaques developed antibodies to p27 and the Env glycoprotein (Fig. 10A). At necropsy, we could not detect the presence of immunoprecipitating antibodies from macaques inoculated with either $SHIV_{Vif5A}$ or $SHIV_{VifHCCH(-)}$ (Fig. 10B). A macaque inoculated

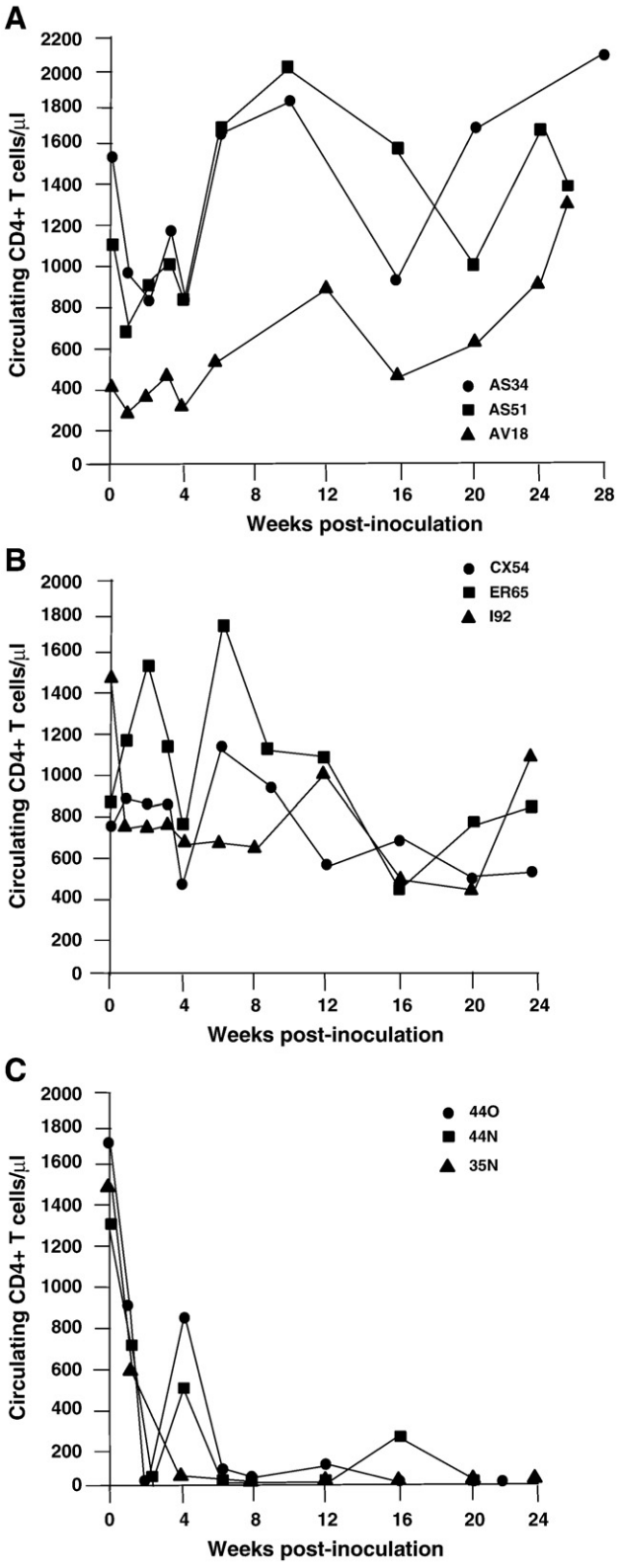

Fig. 7. Circulating $CD4^+$ T cell levels in macaques inoculated with $SHIV_{VifHCCH(-)}$, $SHIV_{Vif5A}$, and $SHIV_{KU\text{-}2MC4}$. Panel A. The levels of circulating $CD4^+$ T cells in three macaques (AS34, ●; AS51, ■; and AV18, ▲) following inoculation with $SHIV_{VifHCCH(-)}$. Panel B. The levels of circulating $CD4^+$ T cells in three macaques (CX54, ●; ER65, ■; and I92, ▲) following inoculation with $SHIV_{Vif5A}$. Panel C. The levels of circulating $CD4^+$ T cells in three macaques (44O, ●; 44 N, ■; 35 N, ▲) following inoculation with $SHIV_{KU\text{-}2MC4}$.

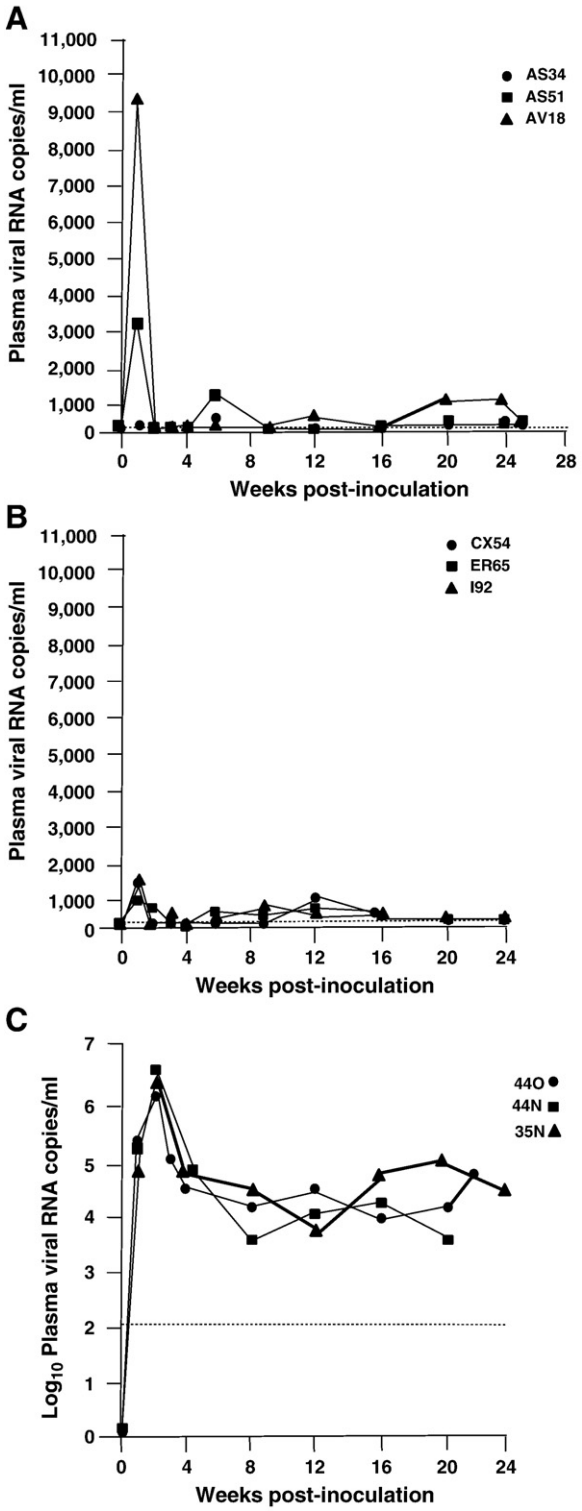

Fig. 8. Plasma viral loads in macaques inoculated with $SHIV_{VifHCCH(-)}$, $SHIV_{Vif5A}$, and $SHIV_{KU\text{-}2MC4}$ as determined by real time quantitative PCR. Panel A. Plasma viral loads in three macaques (AS34, ●; AS51, ■; and AV18, ▲) following inoculation with $SHIV_{VifHCCH(-)}$. Panel B. Plasma viral loads in three macaques (CX54, ●; ER65, ■; and I92, ▲) following inoculation with $SHIV_{Vif5A}$. Panel C. The plasma viral loads in three macaques (44O, ●; 44 N, ■;35 N , ▲) following inoculation with $SHIV_{KU\text{-}2MC4}$.

with parental $SHIV_{KU\text{-}2MC4}$ (44O) did not develop antibodies to the virus at either time point, which is common for macaques that develop severe $CD4^+$ T cell loss during the acute phase (<4 weeks) following inoculation with a pathogenic X4 SHIV (data not shown).

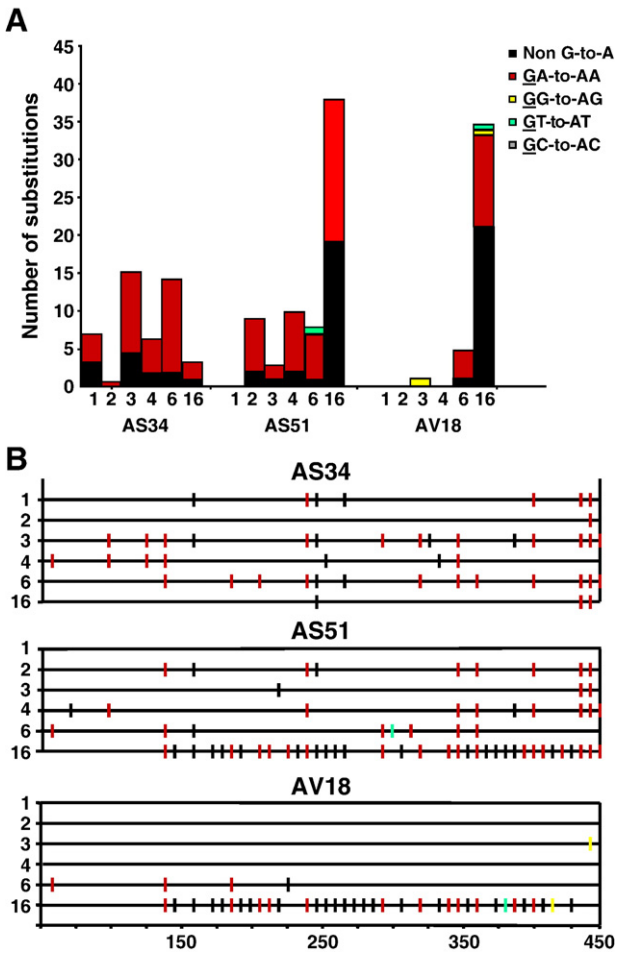

Fig. 9. Analysis of *vif* sequences amplified from DNA isolated from PBMC at various times post-inoculation. Panel A. Quantitative representation of mutations induced in bulk sequences obtained from a 450 base pair fragment of $SHIV_{VifHCCH(-)}$ Vif. Each vertical bar represents the total number of G-to-A substitutions. Each bar is shaded according to the proportion of G-to-A-substitutions the occurred in the context of GA (red), GG (yellow), GT (cyan), or non-G-to-A (black). Panel B. A 450 base pair fragment of the SIV Vif was amplified using DNA isolated from macaque PBMC inoculated with $SHIV_{VifHCCH(-)}$. Mutations from bulk sequence analysis from each macaque are shown. Each mutation is denoted by a vertical line that is color coded with respect to the dinucleotide context: non-G-to-A mutations (black), GA-to-AA (red), GG-to-AG (yellow), or GT-to-AT (cyan).

Histological examination of tissues and viral loads in visceral organs of macaques inoculated with $SHIV_{Vif5A}$ and $SHIV_{VifHCCH(-)}$

Tissues from infected macaques were examined for the presence of lesions consistent with this pathogenic X4 SHIV (Joag et al., 1998). Macaques inoculated with either $SHIV_{Vif5A}$ or $SHIV_{VifHCCH(-)}$ did not exhibit histological lesions in any of the 13 visceral organs examined or in the CNS (data not shown). As the plasma viral loads were significantly less than macaques inoculated with $SHIV_{KU\text{-}2MC4}$, we assessed the tissue distribution of these two viruses in macaques. RNA was isolated from 13 visceral organs from macaques inoculated with $SHIV_{Vif5A}$ and $SHIV_{VifHCCH(-)}$, DNase I treated, and copy numbers determined by real time quantitative RT-PCR. The number of copies is expressed per 10^6 copies of GADPH. The results obtained from macaques inoculated with $SHIV_{VifHCCH(-)}$ are shown in Fig. 11A–C. We found that macaque AS34 had eight tissues (kidney, lung, pancreas, axillary lymph node, inguinal lymph node, spleen, thymus and tonsil) greater than 1000 copies per 10^6 copies of GAPDH (Fig. 11A). Macaque AS51 was found to have two tissues (lung and small intestine) with greater than 1000 copies per 10^6 copies of GAPDH, and macaque AV18 had six tissues (lung, pancreas, axillary lymph node, inguinal lymph node, mesenteric lymph node and spleen) with greater than 1000 copies per 10^6 copies of GAPDH (Fig. 11B–C). Interestingly, the lung had the highest viral copy number in each macaque. In contrast, we were unable to quantify viral RNA from the tissues of macaques that were inoculated with $SHIV_{Vif5A}$ (data not shown). Macaques inoculated with parental $SHIV_{KU\text{-}2MC4}$, 44O and 44 N, had high copy numbers of virus in various tissues (Fig. 11D). Taken together, these results indicate that both $SHIV_{VifHCCH(-)}$ and $SHIV_{Vif5A}$ infections were significantly less widespread compared to macaques inoculated with parental $SHIV_{KU\text{-}2MC4}$.

G-to-A mutations in nef and vpu amplified from DNA of primary and secondary lymphoid organs

A well documented feature of HIV-1Δ*vif* infection is the incorporation of select APOBEC3 proteins into viral particles leading to cytosine deamination during minus strand DNA synthesis (Yu et al., 2003). This results in hypermutation (guanosine to adenosine transitions) of the viral genome and inhibition of virus replication. We examined the number of G-to-A mutations in the *nef* and *vpu* genes amplified from DNA isolated from one primary lymphoid organ (thymus) and two secondary lymphoid organs (ileum of the small intestine and spleen) from the three macaques inoculated with $SHIV_{VifHCCH(-)}$ and one macaque inoculated with $SHIV_{KU\text{-}2MC4}$. We first PCR amplified *nef* and *vpu* sequences from tissue DNA, subcloned and sequenced 15 individual clones. The results showed that there were multiple G-to-A mutations in the *nef* and *vpu* regions amplified from three tissues. The number of G-to-A mutations ranged from 54 to 88 or 1.2% to 1.9% of the total base pairs sequenced (Fig. 12;Table 2). While the percentage of mutations observed in the *vpu* was lower (perhaps reflecting the gradient of mutations from *nef* to *vpu*), the overall number of G-to-A mutations in the context of 5'-T**C** (minus strand) to 5'-C**C** was approximately 2:1 (75 versus 31 mutations) (Fig. 13; Table 3). We plotted the G-to-A mutations obtained from 15 single colony sequences of *nef* and *vpu* amplified from DNA isolated from the ileum of macaques inoculated with $SHIV_{VifHCCH(-)}$ (Figs. 12 and 13). These results showed that many of the G-to-A mutations found in the direct bulk sequencing products were also found in the individually cloned genes (Figs. 12 and 13). Similar to what we reported previously, the majority of the changes were in the context of 5'-T**C** (minus strand) (Tables 2 and 3). Macaque 44O, (inoculated with $SHIV_{KU2\text{-}MC4}$) had very few G-to-A substitutions in *vpu* and *nef* amplified from the same three lymphoid organs, which is similar to other macaques inoculated with this parental virus (unpublished observations). Macaque AV18 yielded the highest number of G-to-A substitutions (88) in the ileum of the small intestine. Taken together these findings suggest that one or more rhA3 proteins have target sequence preference for 5'-T**C** is the major cytidine deaminase at work *in vivo.*

Discussion

There are only a limited number of studies that have analyzed the role of the Vif protein in the SIV or SHIV/macaque models of HIV-1 disease. In the first study, the role of various accessory proteins expressed from $SIV_{mac}239$ was evaluated in terms of the potential to cause disease (Desrosiers et al., 1998). These investigators found that an SIV with deletion of *vif* had only transient viral loads, could only be detected in PBMC for a short period of time and the macaques did not produce antibodies against SIV proteins. In a second study, investigators showed that a *vif*-deleted virus would generate antibody and cellular immune responses if the virus was administered 2–3 times but was not protective against challenge (Sparger et al., 2008). In both studies, the lymphoid and non-lymphoid tissues were not examined for the presence of viral RNA from these *vif-deleted* viruses. Finally, we

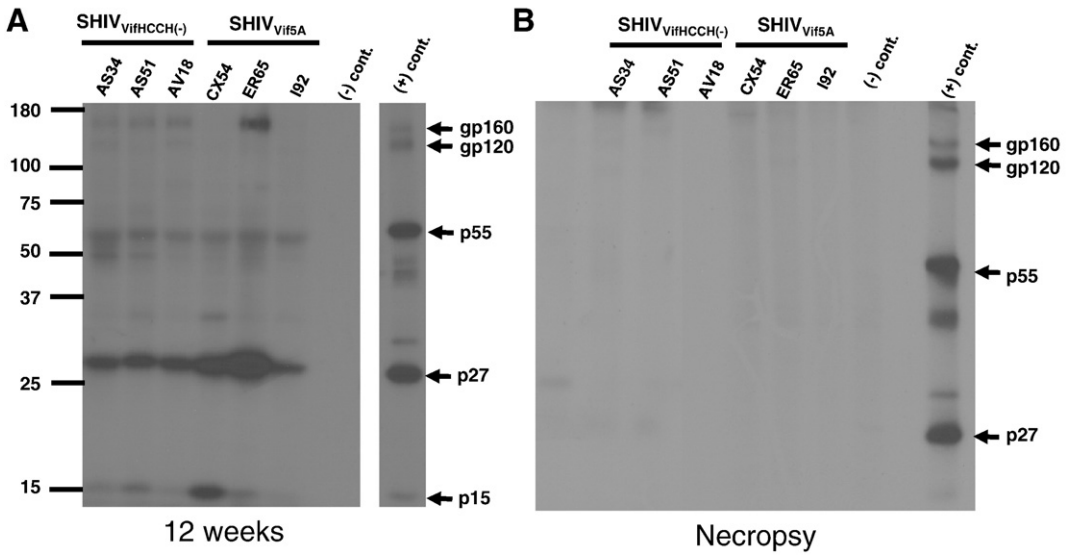

Fig. 10. Macaques inoculated with $SHIV_{Vif5A}$ and $SHIV_{VifHCCH(-)}$ developed antibody responses against each virus at 12 weeks post- inoculation. C8166 cells were inoculated with $SHIV_{KU-2MC4}$ for 5 days, starved for methionine/cysteine and then radiolabeled overnight with ^{35}S-methionine/cysteine. The culture medium was harvested and used in immunoprecipitation reactions with plasma from AS34, AS51, AV18, CX54, ER65, and I92 as described in the Materials and Methods section. The immunoprecipitates were washed with 1× RIPA buffer, boiled in 2× sample reducing buffer, proteins were separated on 12% SDS-PAGE gels, and visualized using autoradiographic techniques. Panel A. SHIV proteins immunoprecipitated with plasma obtained at 12 weeks post-inoculation. The molecular weight standards are shown on the left. Panel B. SHIV proteins immunoprecipitated with plasma obtained at necropsy.

previously showed that the introduction of amino acid substitutions into the SLQYLA domain of Vif (to AAQYLA) resulted in a virus ($SHIV_{VifAAQYLA}$) that did not replicate well in hA3G/F positive cells. However, following inoculation into macaques, the plasma viral loads were lowered from approximately 10^7 copies per ml for wild type virus to approximately 10^5 copies per ml for the $SHIV_{VifAAQYLA}$ during the acute phase of infection (Schmitt et al., 2009). In these macaques, the levels of circulating $CD4^+$ T cells were maintained near pre-inoculation levels and the macaques did not develop histological lesions consistent with a pathogenic X4 SHIV. Sequence analysis of the *vif* gene amplified from the PBMC revealed that the engineered AAQYLA motif had mutated to TAQYLA in two of three macaques. Since serine and threonine are hydroxylated amino acids that differ by a methyl group, it was possible that these Vif proteins may have been "partially" functional *in vivo* to permit limited spread within macaques. Examination of the tissues from these macaques revealed that viral RNA was present in select tissues, and the viral sequences contained low levels of G-to-A substitutions. We also showed that the inoculation of plasma from two of these macaques into a naive macaque did not result in detectable viral loads up to 5 months post-inoculation (Schmitt et al., 2009). Thus, despite the low level of viral replication in cell culture systems, $SHIV_{VifAAQYLA}$ was still capable of significant *in vivo* replication, thus validating the need to examine targeted Vif mutants in macaques.

In the present study, we have extended our *in vivo* studies using SHIV mutants that express either a Vif protein with the first five amino acids of the SLQYLA domain substituted with alanines ($SHIV_{Vif5A}$) or a Vif with the HCCH domain substituted with alanines ($SHIV_{VifHCCH(-)}$). Interestingly, our restriction assays showed that incorporation of rhA3G but not rhA3F resulted in the greatest reduction of replication, which is somewhat different from the results previously reported (Zennou and Bieniasz, 2006). Our results indicate that unlike the parental virus, both mutant viruses incorporated rhA3G while both the parental and mutant viruses incorporated rhA3F into virions. Our analysis of rhA3F and rhA3G stability in the presence of viral genome indicated that rhA3F is stable while rhA3G is degraded. The incorporation of rhA3F into wild type virions is in agreement with a previous study (Zennou and Bieniasz, 2006; Virgen and Hatziioannou, 2007). These paradoxical findings suggest that rhA3F can be incorporated in the presence of SIV_{mac} Vif and that the virus can seemly replicate without the accumulation of lethal mutations. In the former study, these investigators found that rhA3F was resistant to the SIV_{mac} Vif protein. They suggested that rhA3F may not exert a strong negative presence on SIV_{mac} *in vivo* and that the SIV_{mac} Vif may actually permit some degree of mutagenesis by rhA3F. This was supported by analysis of HIV-1 *gag*, *pol*, and *env* for potential editing sites (GG or GA) that would yield a termination codon if mutated. Their analysis revealed that the percentage of GA editing sites leading to termination codons was lower than GG sites in the *gag*, *pol*, and *env*. Analysis of the SIV *gag*, *pol*, *vif*, *vpr*, *vpx*, and *nef* (the SIV genes of our SHIV) also revealed this trend (unpublished observations) yet the mutations observed in the SIV_{mac} *nef* were predominantly in the context of GA and not GG. Whether this was due to lethal GG-to-AG mutations that were subsequently cleared (or not detectable) or whether this was due to rhA3F or other rhA3 proteins is unknown at this time. However, it should be noted that there were differences between our study and the previous study. First, in the previous study the investigators used a HIV-1Δ*vif* genome and we used an SIV-based viral genome with targeted mutations in the *vif*. We showed that replication of $SHIV_{VifSTOP}$ was much lower compared to $SHIV_{Vif5A}$ and $SHIV_{VifHCCH(-)}$ in the presence of rhA3F. Thus, the results of $SHIV_{VifSTOP}$ in our study and HIV-1Δ*vif* in their study are comparable. Our study also shows that our viruses with targeted mutations ($SHIV_{Vif5A}$ and $SHIV_{VifHCCH(-)}$) were restricted less efficiently in the presence of rhA3F compared to $SHIV_{VifSTOP}$, suggesting that the presence of an intact, "crippled" Vif protein can impose some restriction compared to having a Δ*vif* virus. This may relate to the ability of the $Vif_{HCCH(-)}$ and the Vif_{5A} proteins to still bind to rhA3F. Previous studies have defined regions of the HIV-1 Vif that are required for binding various hA3 proteins. Many of these regions are in the amino terminal region of the protein. Previous studies demonstrated that HIV-1 Vif residues ^{40}YRHHY^{44} and ^{12}QVDRMR^{17} are important for the interaction with hA3G and hA3F/C, respectively (Russell and Pathak, 2007; Mehle et al., 2007). In a more recent study, a conserved YXXL domain at residues 69–72 of the HIV-1 Vif was found to be important for the interaction of Vif with hA3G, hA3F and hA3C (Pery et al., 2009). While the ^{12}QVDRMR^{17} and ^{40}YRHHY^{44} are not conserved in the SIV_{mac}239 Vif, there is a lysine at position 27 of the SIV_{mac} Vif that is required for interaction with rhA3G (Chen et al., 2009; Dang et al., 2009). The YWGL domain of the HIV-1 Vif is also

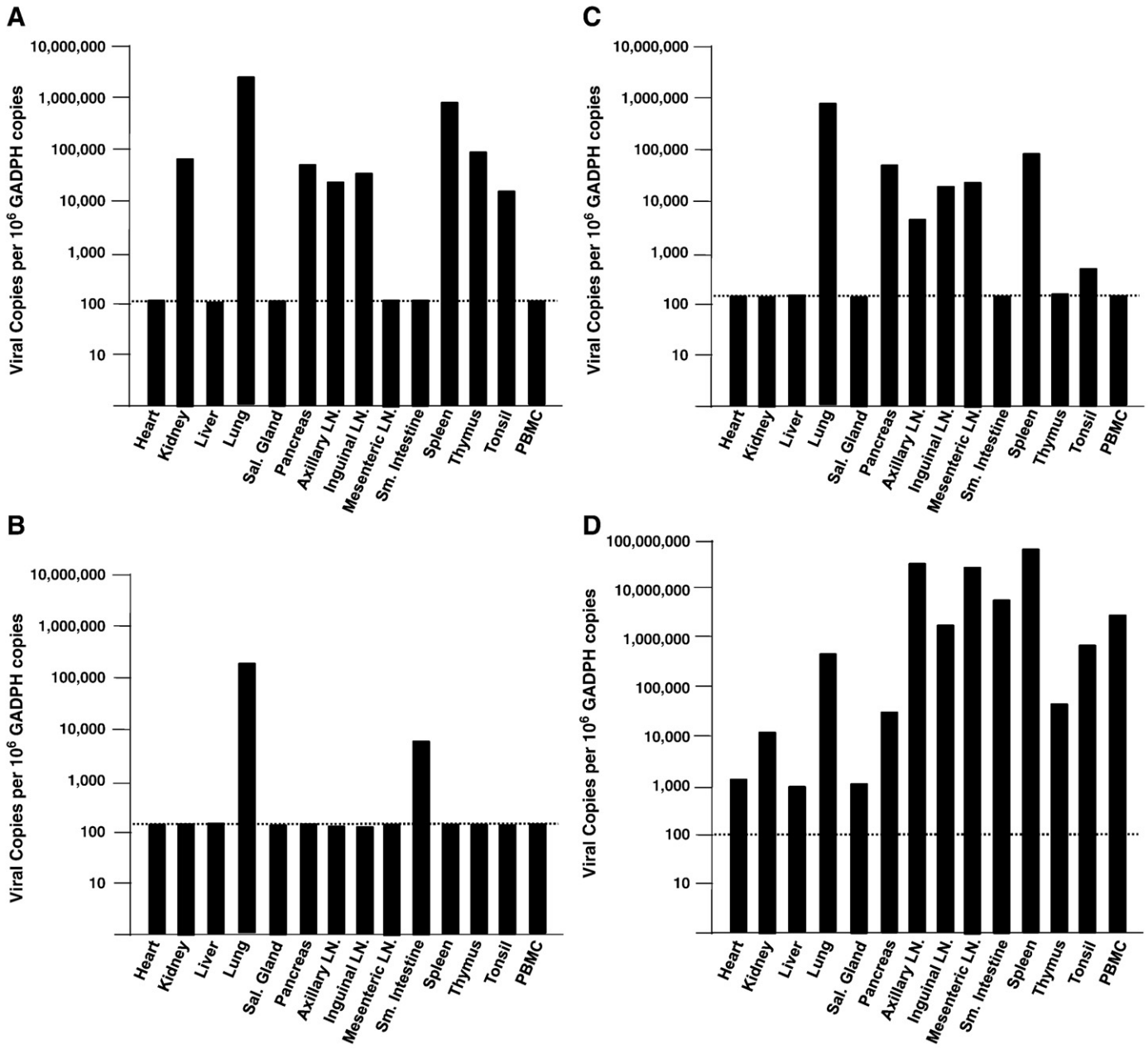

Fig. 11. Comparison of viral copy numbers in the visceral tissues of macaques inoculated with $SHIV_{VifHCCH(-)}$ and $SHIV_{KU\text{-}2MC4}$. RNA was isolated from different visceral organs of macaques inoculated with $SHIV_{VifHCCH(-)}$ or $SHIV_{KU\text{-}2MC4}$, DNase I treated to remove residual DNA and used in real time quantitative RT-PCR using oligonucleotide primers specific for *gag* as described in Materials and methods. The levels of viral RNA are shown per 10^6 copies of GADPH RNA. Panels A–C. The results of the real time quantitative RT-PCR using RNA isolated from tissues of macaques AS34 (Panel A), AS51 (Panel B) and AV18 (Panel C), which were inoculated with $SHIV_{VifHCCH(-)}$. Panel D. The results of the real time quantitative RT-PCR using RNA isolated from tissues of macaque 44O, which was inoculated with $SHIV_{KU\text{-}2MC4}$. The dotted line represents the limits of detection of this assay.

conserved in the SIV Vif (as YWHL). Thus, it is possible that the Vif proteins with targeted amino acid substitutions may still bind and incorporate rhA3F into virus particles but may be inefficient in deamination because of its association with Vif. A second difference in the two studies is the hypermutation assay used to analyze the percentage of G-to-A changes in the genome. While the previous study showed that rhA3F caused G-to-A hypermutation at levels higher than rhA3G, we found that rhA3F produced little hypermutation in the viral genome. In the previous study, these investigators used a VSV pseudotyped HIV-1 vector with the *vif* deleted as well as other genes and analyzed hrGFP sequences. In our system, we used complete SIV viral genomes expressing the Vif mutants.

One goal of these studies was to determine if $SHIV_{Vif5A}$ was effectively controlled by macaques during the primary phase of infection or if viral variants would emerge that would permit limited replication in macaque tissues. Our results indicate that following inoculation of $SHIV_{Vif5A}$ into macaques, there was a further reduction of plasma viral loads compared to $SHIV_{VifAAQYLA}$ (Schmitt et al., 2009). The mean peak plasma virus load (week 1) was 1.3×10^3 viral copies per ml or approximately 4000-fold lower than parental $SHIV_{KU\text{-}2MC4}$. However, following this initial burst of replication, viral RNA from macaques inoculated with $SHIV_{Vif5A}$ was near or below the limits of detection for this assay (~180 copies). It should be noted that the virus was not completely eliminated because viral RNA was occasionally detected in the plasma throughout the 6-month infection using nested RT-PCR (data not shown). At necropsy, the number of copies of viral RNA could not be quantified from various organs of these macaques (detection limit 180 copies) but could be detected by

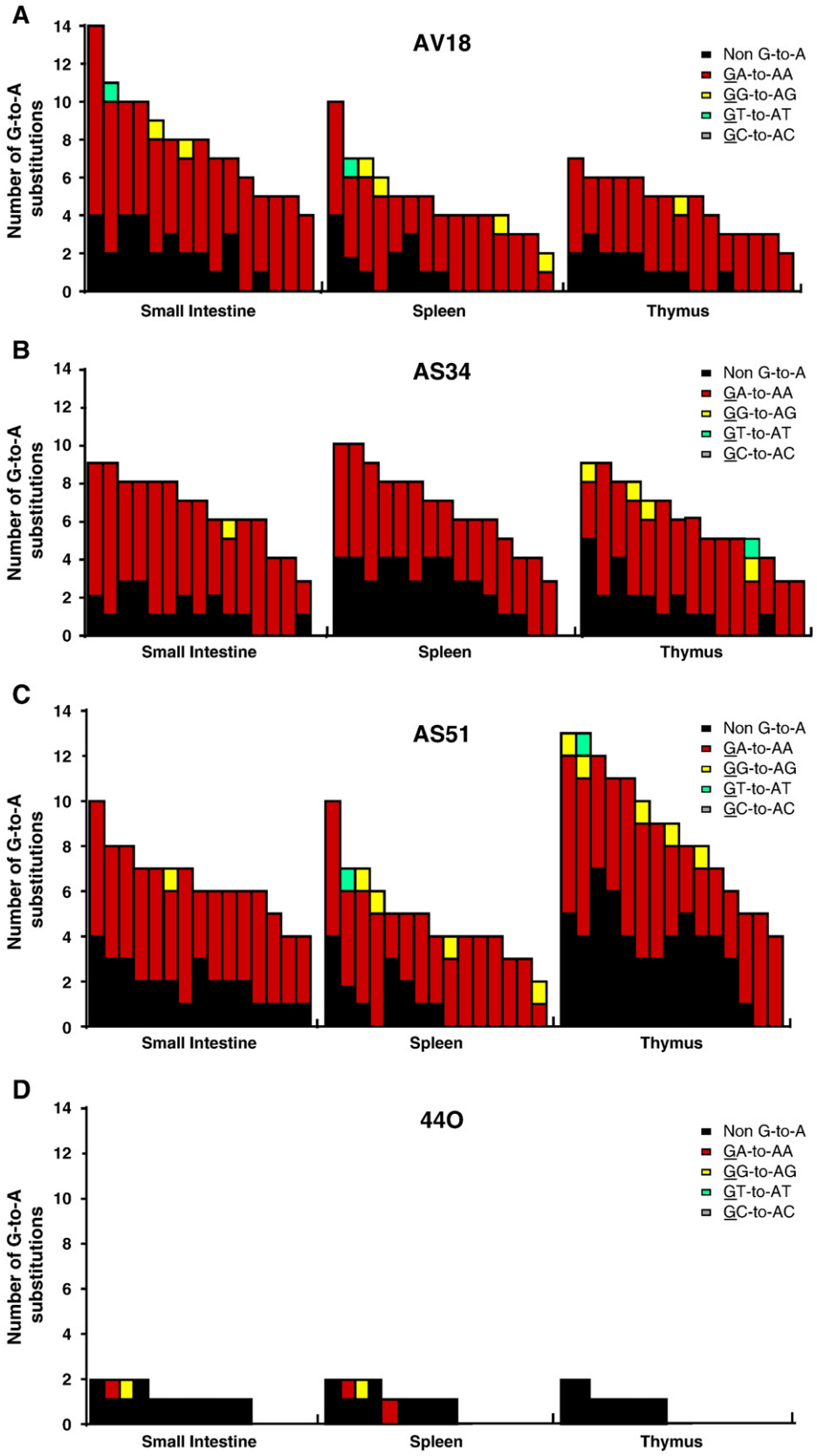

Fig. 12. Quantitative assessment of mutations in the *nef* gene. Panels A–D. A 300 base pair fragment of *nef* was amplified using DNA isolated from the small intestine (ileum), spleen and thymus of macaques inoculated with $SHIV_{VifHCCH(-)}$. Mutations obtained using sequence analysis of fifteen independent clones from each macaque is shown. Each vertical bar represents an individual clone, whose height represents the total number of substitutions. Each bar is shaded according to the proportion of G-to-A-substitutions the occurred in the dinucleotide context: non-G-to-A (black), GA (red), GG (yellow), GT (cyan), or GC (gray). Panels E–G. Hypermutation plot illustrating the G-to-A and non-G-to-A substitutions in the clones from the ileum amplified DNA. Each mutation is denoted by a vertical line that is color coded with respect to the dinucleotide context: non G to A (black), GG to AG (yellow), GA to AA (red), GT to AT (cyan), and GC to AC (gray).

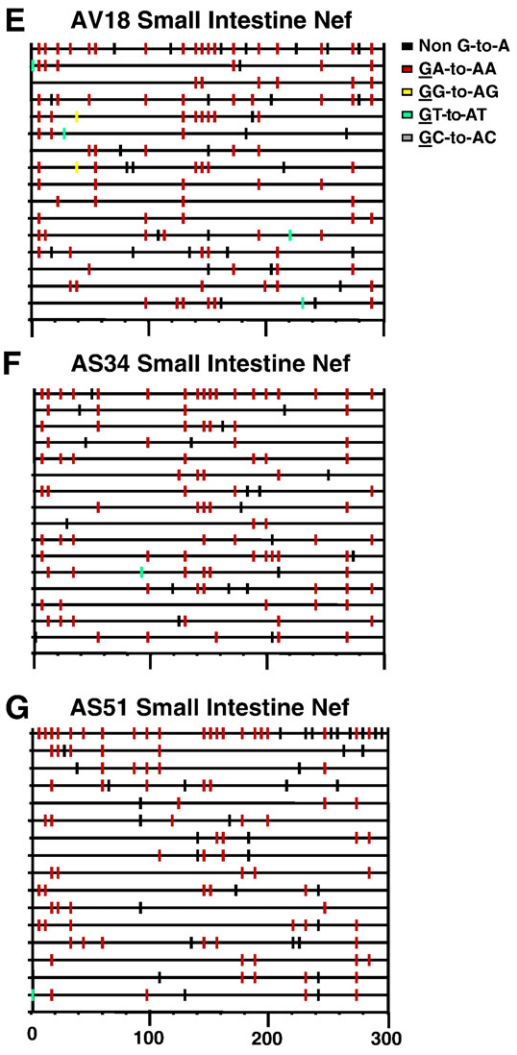

Fig. 12 (*continued*).

nested RT-PCR. We were unable to detect the virus in PBMC by 3 weeks post-inoculation and were unable to amplify the *nef* gene at necropsy for sequence analysis. While the results presented here may be predicted based on studies in cell culture systems, these results demonstrate for the first time that a primate lentivirus expressing a Vif protein with only targeted mutations in a critical domain can be completely controlled by the host. Taken together, these results indicate that the $SHIV_{Vif5A}$ replicated similarly to a virus that does not express a functional Vif protein (Desrosiers et al., 1998).

No studies have analyzed the role of the Zn^{++} binding domain of Vif *in vivo*. Previous studies have shown that this domain is critical to Vif function, interacting with Cul 5 of the Cul 5/ElonginB/C/Rbx E3 ligase (Luo et al., 2005; Xiao et al., 2007). Our results showed that these macaques had slightly higher initial viral loads at 1 week post-inoculation than macaques inoculated with $SHIV_{Vif5A}$ but that the virus was effectively controlled by the macaques by 3 weeks post-inoculation. Similar to our previous study, the majority of the G-to-A mutations were in the context of 5'-T**C** (minus strand) and not 5'-C**C**. In addition, we observed that the majority of the G-to-A changes found in the *vif* gene amplified from PBMC DNA occurred during the first weeks of infection. This correlated well with the plasma viral loads which indicated the viral replication primarily occurred during this time period.

Taken together, our results show that abolishing the SLQYLA domain of Vif may be more detrimental to the virus *in vivo* than the HCCH domain. These data bring up the question, "Why were we able to quantify viral RNA from tissues of macaques inoculated with $SHIV_{VifHCCH(-)}$ but not $SHIV_{Vif5A}$?" While the answer is unknown, several possibilities exist. First, the virus may have initially replicated in cells expressing active rhA3 proteins and incorporated one or more rhA3 proteins into the viral progeny. In the next round of replication the genome was mutated but not to the extent that RNA polymerase II could not transcribe viral RNA. Second, there may be a tissue/cellular reservoir for virus replication that do not express the rhA3 proteins that would restrict the crippled $SIV_{mac}239$ Vif protein. We previously showed using immunohistochemistry that rhA3G was not expressed in all cell types in the brain and kidneys (Hill et al., 2006, 2007). Finally, during the initial rounds of replication and potential deamination, G-to-A mutations may have led to compensating mutations that made the viral Vif partially functional. The latter scenario is not likely as our sequence analysis did not identify consensus mutations in either the $SHIV_{Vif5A}$ or $SHIV_{VifHCCH(-)}$-inoculated macaques.

As previous studies showed that antibody responses were not generated with a single inoculation of *vif-deleted* viruses (Desrosiers et al., 1998; Sparger et al., 2008), we determined if a single inoculation of either virus would result in an antibody response against viral proteins. Comparison of the antibody responses from macaques inoculated with either $SHIV_{VifHCCH(-)}$ or $SHIV_{Vif5A}$ shows that at 12 weeks post-inoculation macaques had developed antibody responses against the virus but these were undetectable at necropsy. This would argue that the viral RNA detected in tissues at necropsy may not have been translated into viral proteins. This would also suggest that infectious virus was cleared by the macaque and that antigenic stimulation through viral proteins did not occur. However, this study provides evidence that such viruses containing site-directed mutations in *vif* could be used to "prime" the immune system and suggests that such a virus could be useful in a prime-boost strategy. It will be of interest to determine if multiple inoculations will result in stronger immune responses (both humoral and cellular) and a further reduction of viral loads with increasing inoculations. If successful, it will be of interest to determine if the immune responses are protective against challenge. While the use of live attenuated lentiviruses has led to useful information concerning the role of accessory genes in replication of the virus *in vivo*, the use of such vaccines has several underlying risks (Koff et al., 2006). First, these vaccines have relied on the deletion/disruption of accessory genes (*nef, vpu, vpx/vpr*) that enhance replication but are not absolutely required for replication *in vivo*. For this reason these viruses can select for compensating mutations that ultimately result in the virus

Table 2
Results of sequence analysis of *nef* amplified from the thymus, ileum, and spleen.

Animal Tissue	[a]Total number of bases sequenced	Total # of G-to-A mutations/percent G-to-A mutations of bases sequenced	Number and context of cytidine deamination		
			5'-GA	5'-GG	% 5'-GA to GG
AS34					
Thymus	4500	71/1.6	67	4	94.3
Spleen	4500	61/1.4	59	2	96.7
Ileum	4500	83/1.8	82	1	98.7
AS51					
Thymus	4500	75/1.7	69	6	92.0
Spleen	4500	62/1.4	62	0	100
Ileum	4500	66/1.5	65	1	98.4
AV18					
Thymus	4500	54/1.2	54	0	100
Spleen	4500	58/1.3	54	4	93.1
Ileum	4500	88/2.0	86	2	97.7

[a] A 300 base fragment corresponding to the 5' end of *nef* was amplified, cloned and 15 separate clones sequenced.

becoming pathogenic (Baba et al., 1995; 1999). The second problem is the risk of recombination of the viral genome to yield a pathogenic virus (Kim et al., 2005). A vaccine based on a "crippled Vif" that allows for limited replication resulting in G-to-A substitutions and inactivation of the virus should prevent the scenarios discussed above. It would be of interest to determine if inoculation of macaques with two

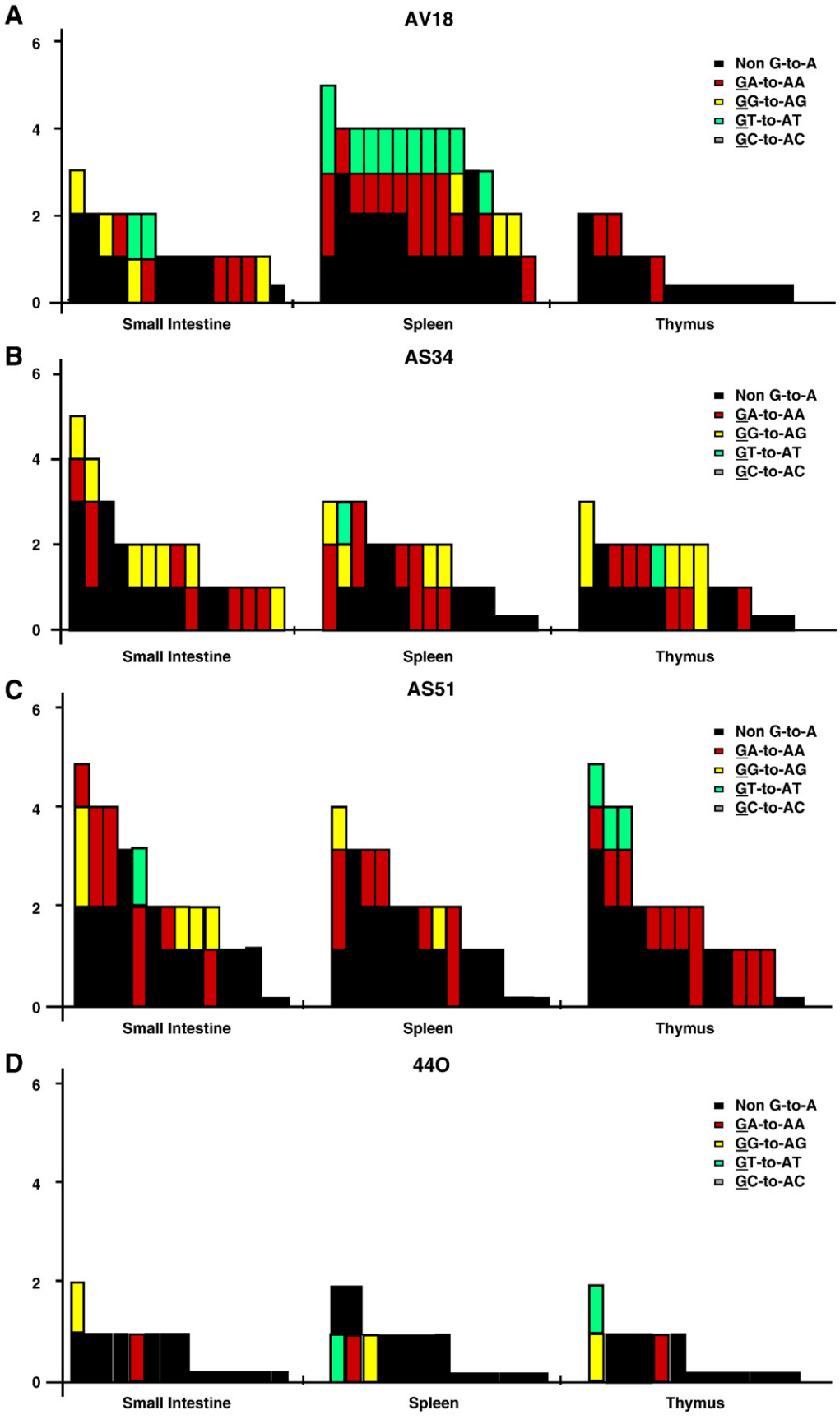

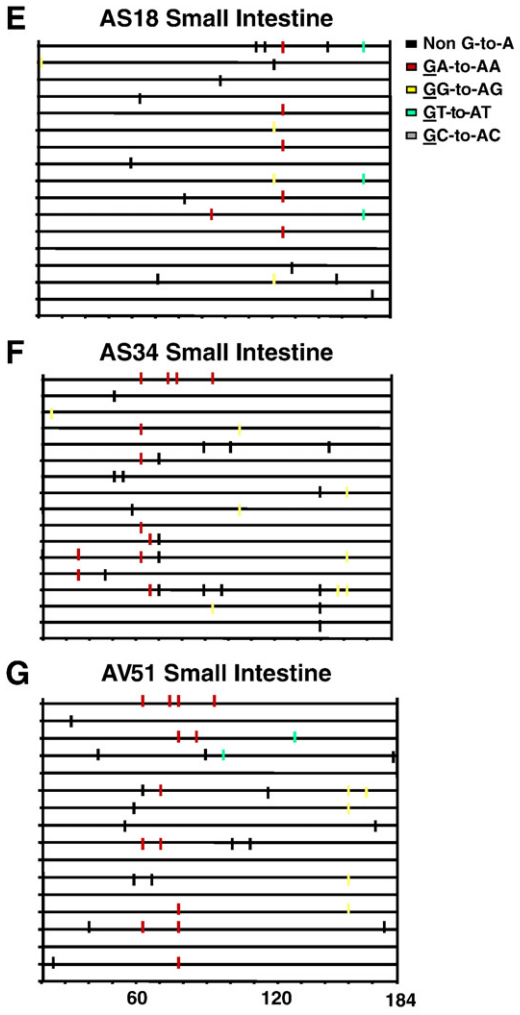

Fig. 13. Quantitative assessment of mutations in the *vpu* gene. Panels A-D. A 184 base pair fragment of *vpu* was amplified using DNA isolated from the ileum, spleen and thymus of macaques inoculated with $SHIV_{VifHCCH(-)}$ and one macaque inoculated with $SHIV_{KU\text{-}2MC4}$. Substitutions were determined using sequence analysis of fifteen independent clones from each macaque are shown. Each mutation is denoted by a vertical bar that is color coded with respect to the dinucleotide context: non-G to A (black), GG to AG (yellow), GA to AA (red), GT to AT (cyan), and GC to AC (gray). Panels E-G. Hypermutation plot illustrating the G-to-A and non-G-to-A substitutions in the clones obtained from the small intestine (ileum) amplified DNA. Each mutation is denoted by a vertical line that is color coded with respect to the dinucleotide context: non G to A (black), GG to AG (yellow), GA to AA (red), GT to AT (cyan), and GC to AC (gray).

viruses, one harboring a mutation in *vif* and another having a mutation in another accessory gene such as *nef* can recombine *in vivo* to generate a wild type virus causing $CD4^+$ T cell loss and disease prior to the virus accumulating G-to-A mutations.

Materials and methods

Cells, plasmids, and viruses

The C8166 and SupT1 lymphocyte cell lines were used for transfections of full-length SHIVs and as indicator cells to measure infectivity and cytopathicity of the viruses used in this study. Both cell lines were maintained in RPMI-1640, supplemented with 10 mM Hepes buffer pH 7.3, 2 mM glutamine, 5 μg per ml gentamicin, 100 units/μg penicillin-streptomycin and 10% fetal bovine serum (R10FBS). Rhesus macaque PBMCs were obtained from uninfected animals and isolated on Ficoll/Hypaque gradients for p27 growth curves. The 293 and TZM-bl cell lines were maintained in Dulbecco's minimal essential medium (DMEM) with 10% fetal bovine serum and the antibiotics described above. The derivation of $SHIV_{KU\text{-}2MC4}$ has been previously described (Joag et al., 1998). The pcDNA3.1(+)-rhesus APOBEC3G-HA and pcDNA3.1(+)-rhesus APOBEC3F-V5 were kindly provided by Dr. Nathaniel Landau (New York University School of Medicine, New York, New York).

Construction of $SHIV_{Vif5A}$, $SHIV_{VifHCCH(-)}$ and $SHIV_{VifSTOP}$

For the construction of $SHIV_{VifHCCH(-)}$, the *Pac*I/*Sph*I fragment (nucleotides 5132 to 6452) from the p5'-SHIV4 was subcloned into the pGEM-3Zf (+) vector (Promega). The histidine to alanine substitution at position 110 of Vif was introduced using oligonucleotides (only sense strand shown) 5'-GCAGACATTTTACTGGCTAGCACT-TATTTCC-3'. The cytidine to alanine substitution at position 116 of Vif was introduced using oligonucleotides (only sense strand shown) 5'-GCACTTATTTCCCTGCCTTTACAGCGGGAG-3'. The cysteines at positions 134 and 135 of Vif were substituted for alanines using the oligonucleotides (only sense strand shown) 5'-CAACTGCTGTCTGCCGC-CAGGTTCCCG-3'. The histidine to alanine substitution at position 144 of Vif was introduced using oligonucleotides (only sense strand shown) 5'-GGTTCCCGAGAGCTGCTAAGTACCAGGTACC-3'. All substitutions were made using the Quik-Change Mutagenesis Kit (Stratagene) following the manufacturer's instructions. The resulting *Pac*I/*Sph*I fragment was digested, isolated, and subcloned into full-length $SHIV_{KU\text{-}2MC4}$. The resulting plasmid was sequenced to ensure that the desired mutations were introduced as expected.

For the construction of $SHIV_{Vif5A}$, the *Pac*I/*Sph*I fragment (nucleotides 5132 to 6452) from full-length $SHIV_{KU\text{-}2MC4}$ was subcloned into the pGEM-3Zf (+) vector. The serine and leucine at positions 147 and 148 were substituted for alanines using the oligonucleotides (sense strand shown) 5'-CCAGGTACCAGCCGCACAGTACTTAGCAC-3'. The glutamine and tyrosine at positions 149 and 150 were substituted for alanines using the oligonucleotides (sense strand shown) 5'-CCAGGTACCAGCCGCAGCGGCCTTAGCACTGAAAGTAGTAAGC-3'. The leucine at position 151 was substituted for an alanine using the oligonucleotide (sense strand shown) 5'-GGTACCAGCCGCA-GCGGCCGCAGCACTGAAGTAGTAAGCG-3'. All substitutions were made using the Quik-Change Mutagenesis Kit (Stratagene) following the manufacturer's instructions and virus constructed and prepared as described above.

For the construction of $SHIV_{VifSTOP}$, the tyrosine and leucine at amino acid positions 28 and 29 were engineered to have stop codons using site-directed mutagenesis in order to produce a full-length SHIV

Table 3
Results of sequence analysis of *vpu* amplified from the thymus, ileum, and spleen.

Animal Tissue	[a]Total number of bases sequenced	Total # of G-to-A mutations/percent G-to-A mutations of bases sequenced	Number and context of cytidine deamination		
			5'-GA	5'-GG	% 5'-GA to GG
AS34					
Thymus	2760	13/0.47	6	6	50.0
Spleen	2760	15/0.54	10	4	71.4
Ileum	2760	15/0.54	8	7	53.3
AS51					
Thymus	2760	14/0.51	11	0	100
Spleen	2760	9/0.33	7	2	77.8
Ileum	2760	15/0.54	9	5	64.2
AV18					
Thymus	2760	3/0.12	3	0	100
Spleen	2760	30/1.09	16	3	84.2
Ileum	2760	11/0.40	5	4	55.5

[a] A 184 base fragment corresponding to *vpu* was amplified, sub-cloned and 15 independent clones sequenced.

that does not express a functional Vif protein. The oligonucleotide used to introduce these mutations was 5'-GCCTCATTAAAATAGTAG-AAATATAAAACTAAAG-3' (only sense strand shown). The substitutions were made using the Quik-Change Mutagenesis Kit (Stratagene) following the manufacturer's instructions. The resulting *Pac*I/*Sph*I fragment was digested, isolated, and subcloned into full-length $SHIV_{KU\text{-}2MC4}$. The resulting plasmid was sequenced to ensure that the desired mutations were introduced as expected. For all three viruses, the plasmids containing the full-length genomes were transfected into SupT1 cells as previously described (Stephens et al., 2002; Hout et al., 2005). Stocks of $SHIV_{VifHCCH(-)}$, $SHIV_{Vif5A}$, and $SHIV_{VifSTOP}$ were prepared, tittered on SupT1 cells, and stored at −86 °C.

Analysis of the replication of $SHIV_{Vif5A}$ and $SHIV_{VifHCCH(-)}$ in APOBEC3G/F positive and negative cells

C8166 (A3G/F positive) and SupT1 (A3G/F negative) cells were inoculated with equivalent levels (25 ng) of parental $SHIV_{KU\text{-}2MC4}$, $SHIV_{Vif5A}$, $SHIV_{VifHCCH(-)}$, $SHIV_{VifAAQYLA}$, or $SHIV_{VifSTOP}$ for 4 h at 37 °C. For rhesus PBMC, cells were isolated on Ficoll-Hypaque gradients, stimulated for 48 h in R10FBS supplemented with concanvalin A (10 μg/ml) and interleukin-2 (IL-2; 50 ng/ml). The cells were washed, and inoculated with virus (25 ng) incubated in R10FBS containing interleukin-2 (50 ng/ml) for 4 h. At 4 h, cells were centrifuged, washed 3 times to remove the inoculum and incubated in fresh medium (medium for the rhesus PBMC also contained 50 ng/ml IL-2) at 37 °C for up to 15 days. Aliquots of culture supernatants were obtained at 0, 1, 3, 5, 7, 9, 11, 13, and 15 days post-inoculation and the levels of p27 assessed using a commercial p27 antigen capture kit (Zeptometrix).

APOBEC3G/F incorporation assays

Plasmids containing the genomes of the viruses (derived from $SHIV_{KU\text{-}2MC4}$) expressing each of the mutant Vif proteins described above were co-transfected into 293 cells using PEI transfection reagent (Ex-Gen 500, Fermentas) along with plasmids expressing either HA-rhA3G or V5-rhA3F. At 48 h, virus containing supernatants were harvested and clarified by low speed centrifugation. The clarified supernatant was then subjected to ultracentrifugation to pellet the virus (SW41 rotor, 247,000*g*, 1 h). The pellet was resuspended in PBS (pH 7.4) and layered on a 20/60% sucrose step gradient and again subject to ultracentrifugation (SW55Ti, 247,000*g*, 1 h). The virus (at the interface) was harvested, pelleted again by ultracentrifugation described above, and resuspended in 200 μl of 1× PBS (pH 7.4). An aliquot was saved to determine the p27 content by antigen capture assay (Zeptometrix). The remaining sample was boiled in sample reducing buffer. Equivalent amounts of p27 were loaded on a 12% SDS-PAGE gel and transferred to PVDF membranes. APOBEC3 proteins were detected by Western blotting using an antibody directed against either the HA tag (HA-probe; Santa Cruz) or V5 tag (Clone V5-10; Sigma). Blots were stripped in 1× stripping buffer (62.5 mM Tris–HCl, pH 6.8 and 2% SDS) and reprobed using a rabbit polyclonal antibody specific for p27. As a control, plasmids expressing either rhA3G or rhA3F were transfected into 293 cells using PEI transfection reagent (Ex-Gen500, Fermentas). At 48 h post-transfection, cells were lysed in 1× RIPA and the nuclei were removed. Whole protein was precipitated with methanol and resuspended in 2× sample reducing buffer. Normalized to β-actin, the samples were run on a 12%-SDS-PAGE gel, and probed with the antibodies stated above.

Stability of rhA3G and rhA3F in the presence of SHIV genomes

We determined if rhA3G or rhA3F were stable in the presence of $SHIV_{KU\text{-}2MC4}$, $SHIV_{VifHCCH(-)}$, $SHIV_{Vif5A}$, or $SHIV_{VifSTOP}$. Full-length mutated SHIVs were co-transfected in a 2:1 ratio with either APOBEC3G-HA or APOBEC3F-V5 using polyethylenimine transfection reagent (PEI, Fermentas). Twenty-four hours post-transfection, the supernatant was removed and the cells were harvested and lysed using 1× RIPA (50 mM Tris–HCl, pH 7.5; 50 mM NaCl; 0.5% deoxycholate; 0.2% SDS; 10 mM EDTA). Following lysis, the nuclei were removed by microcentrifugation at 14,000 rpm for 15 min. The protein was precipitated using methanol, resuspended in 2× sample reducing buffer, and boiled for 5 min. Proteins were separated on a 10% SDS-PAGE gel and probed using commercially available rabbit polyclonal HA antibody (HA-probe, Santa Cruz) for rhA3G-HA or mouse monoclonal V5 antibody (Clone V5-10, Sigma) for rhA3F. All samples were normalized to the amount of beta-actin protein using a mouse monoclonal antibody (Novous Biologicals) specific for beta-actin.

Hypermutation assays in the presence of rhA3G or rhA3F

Hypermutation of various SHIVs in the presence of rhesus APOBEC3G/F 293 cells were transfected with $SHIV_{KU\text{-}2MC4}$, $SHIV_{VifHCCH(-)}$, $SHIV_{Vif5A}$, or $SHIV_{VifSTOP}$ in the presence of either rhA3G or rhA3F using PEI transfection reagent (Ex-Gen, Fermentas). Twenty-four hours post-transfection, cells were washed and fresh DMEM was added. After 48 h, the supernatant containing virus was subjected to low speed centrifugation. The resulting supernatant was DNase-I-treated (Fermentas) at 37 °C for 30 min to eliminate any trace of plasmid carry-over from the initial transfection. The DNase-I-treated supernatant was titrated on TZM-bl cells to both assess infectivity and hypermutation. Twenty-four hours post-infection, total DNA cellular DNA was harvested and extracted using the DNeasy kit and the manufacturer's instructions (Qiagen). The DNA was used in a nested DNA polymerase chain reaction to amplify a 300 base pair fragment of *nef*. The PCR reaction was carried out using rTaq, the manufacturer's instructions (Takara), and the oligonucleotides listed below. 1 μl of the first PCR product was added to a nested reaction. The PCR reactions were performed using an Applied Systems 2720 Thermal Cycler with the following thermal profile: 95 °C for 2 min, 1 cycle; 95 °C for 30 s, 48 °C for 30 s, 65 °C for 2 min, 35 cycles; 65 °C for 7 min. The PCR products were separated by electrophoresis, isolated, purified, sequenced and sub-cloned into pGEM-TEasy (Promega) as described below. Fifteen independent clones were sequenced and assessed for each mutant SHIV as described above.

Restriction of Vif mutants on rhA3G or rhA3F

We determined the effect of the Vif mutants on the suppression of rhA3G and rhA3F. Full-length mutated SHIVs were co-transfected with either rhA3G or rhA3F using PEI transfection reagent (Ex-Gen500, Fermentas). Forty-eight hours post-transfection, the supernatant was harvested and purified by low speed centrifugation. Equivalent amounts of p27 were serially diluted using 10-fold dilutions from 10^1 to 10^6 and used to inoculate TZM-bl cells . Forty-eight hours later, the media was removed, cells washed with 1× PBS and the monolayer fixed using 0.8% formaldehyde-0.25% glutaraldehyde in phosphate-buffered saline (1× PBS). The cells were washed and incubated in a solution for 2 h at 37 °C in 4 mM potassium ferrocyanide, 4 mM potassium ferricyanide, 4 mM magnesium chloride, and 0.4 mg X-gal per ml. The reaction was stopped and the number of $TCID_{50}$ were calculated (Derdeyn et al., 2000; Wei et al., 2000).

Macaques analyzed in this study

Three rhesus macaques (*Macaca mulatta*: CX54, ER65, and I92) were intravenously inoculated with 1 ml of undiluted culture supernatant from SupT1 grown virus stocks (containing 10^4 $TCID_{50}$

per ml). Three additional rhesus macaques (AS34, AS51, and AV18) were inoculated with 10^4 $TCID_{50}$ $SHIV_{VifHCCH(-)}$ (titered in SupT1 cells). The animals were housed in the AAALAC-approved animal facility at the University of Kansas Medical Center. All aspects of the animal studies were performed according to the institutional guidelines for animal care and use at the University of Kansas Medical Center. Heparinized blood was collected weekly for the first 4 weeks, then at 2 week intervals for the next month and at monthly intervals thereafter.

Assays for circulating $CD4^+$ T cells

Changes in the levels of $CD4^+$ T cells after viral inoculations were monitored sequentially by flow cytometric analysis (BD Biosciences). T cell subsets were labeled with a commercially available anti-CD3/CD4/CD8 mixture. T cell subsets from a normal uninfected macaque were always performed at the same time to serve as a control for the flow cytometry analysis.

Processing of tissue samples at necropsy

At the time of euthanasia (26 or 28 weeks), all macaques in this study were anesthetized by administration of 10 mg/kg ketamine (IM) followed by intravenous administration of sodium phenobarbital at 20–30 mg/kg. At the time of necropsy, all macaques were in a healthy condition. A laparotomy was performed. The animal was exsanguinated by aortic canulation and perfused with 1 l of cold Ringer's saline. Lymphoid and non lymphoid tissues (heart, kidneys, liver, lungs, mesenteric, inguinal and axillary lymph nodes, pancreas, salivary gland, small intestine, spleen, thymus, and tonsils) were obtained and aliquots of tissue snap frozen for DNA and RNA assays. Aliquots of lymphoid tissues were immersed in HBSS to quantify levels of infectious virus in tissues using infectious centers assays with SupT1 cells.

Sequence analysis of the vif, nef, and vpu genes

To determine the stability of the mutations that were introduced into *vif* and assess whether these macaques acquired G-to-A mutations, the *vif, nef,* and *vpu* genes were amplified from either PBMCs at different time points during infection (*vif*) or from several tissue DNA samples taken at necropsy (*nef* and *vpu*) that were positive for viral RNA. One hundred nanograms of extracted genomic DNA was used in a nested DNA polymerase chain reaction (Takara, Madison, WI) following the manufacturer's instructions. The oligonucleotides employed during the first round to amplify *vif* were 5'-GGCTAAAATTATCAAAGATTATGGAGG-3' (sense) and 5'-GGTGACATCCCTTGTTCATCATGCC-3' (antisense), which corresponds to bases 5326–5352 and 5984–6008, respectively. The nested oligonucleotides were 5'-GGAGGAGGAAAAGAGGTGGATAGCAGTTCCC-3' (sense) and 5'-CCAGTATTCCCAAGACCTTTGCC-3' (antisense), which corresponds to bases 5348–5378 and 5963–5985, respectively. The oligonucleotides used during the first round to amplify the *nef* gene were 5'-GGTGGAGCTATTTCCATGAGG-3' (sense) and 5'-GTCTTCTTGGACTGTAATAAATCCC-3' (antisense), which corresponds to bases 9445–9465 and 9832–9856, respectively. The nested oligonucleotides were 5'-CCATGAGGCGGTCCAGGCAGTCTAGAG-3' (sense) and 5'-CCTCCCAGTCCCCCCTTTTC-3' (antisense), which corresponds to bases 9458–9484 and 9814–9833, respectively. The oligonucleotides used during the first round to amplify the *vpu* gene were 5'-CCTAGACTAGAGCCCTGGAAGCATCC-3' (sense) and 5'-GTACCTCTGTATCATATGCTTTAGCAT-3' (antisense), which corresponds to bases 6486–6511 and 7034–7061, respectively. The nested oligonucleotides used were 5'-TTAGGCATCTCCTATGGCAGGAAGAAG-3' (sense) and 5'-CACAAAATAGAGTCCTGGTTGCTTCCT-3' (antisense), which corresponds to bases 6597–6623 and 7001–7027, respectively.

For sequence analysis, the PCR products from three separate PCR reactions were pooled and separated by electrophoresis in a 1.5% agarose gel, isolated, and each PCR reaction directly sequenced. Cycle sequencing reactions using the BigDye Terminator Cycle Sequencing Ready Reaction Kit with AmpliTaq DNA polymerase, FS (PE Applied Biosystems, Foster City, CA) sequence detection was conducted with an Applied Biosystems 377 Prism XL automated DNA sequencer and visualized using the ABI Editview program. Sequences were compared to the sequence of $SHIV_{KU\text{-}2MC4}$. A total of 615 nucleotides were analyzed from *vif*, 300 nucleotides analyzed from *nef*, and 184 nucleotides from *vpu* using the SE Central Software package. In order to isolate and analyze single sequences, bulk PCR reactions were subcloned into the pGEM-T Easy (Promega) cloning vector. Fifteen clones were selected, sequenced as described above, and analyzed to assess the number of G-to-A substitutions that occurred.

Plasma virus loads

Plasma viral RNA loads were determined on RNA extracted from 1 ml of EDTA-treated plasma. Virus was pelleted using ultracentrifugation (Beckman SW55Ti, 250,000*g*, 2 h) and RNA extracted using the Qiagen viral RNA kit (Qiagen). RNA samples were analyzed by real-time RT-PCR using *gag* primers and a 5'FAM and 3'TAMRA labeled Taqman probe that is homologous to the SIV *gag* gene as previously described (Hofmann-Lehmann *et al.*, 2000). Standard curves were prepared using a series of six ten-fold dilutions of viral SIV *gag* RNA of known concentration. The sensitivity of the assay was 100 RNA equivalents per ml. Samples were analyzed in triplicate and the number of RNA equivalents per ml of plasma were calculated. Viral RNA was also quantified from in visceral tissues using this primer/probe reaction. In order to quantify the amount of viral RNA, GAPDH was used as a control and data is presented as copies per 10^6 GAPDH molecules (Marcario et al., 2008).

Immunoprecipitation assays

To determine if the macaques developed antibodies to SHIV proteins following inoculation, the plasma at 12 weeks and at necropsy was used in immunoprecipitation assays. C8166 cells were inoculated with approximately 10^4 $TCID_{50}$ of $SHIV_{KU\text{-}2MC4}$ for 5 days. The cells were then incubated in methionine/cysteine-free media for 2 h and radiolabeled with 500 μCi of ^{35}Smethionine/cysteine for 15 h. The cells were lysed in 1 ml of 1× RIPA buffer and nuclei were removed by centrifugation. The cell lysates were incubated overnight at 4 °C with 10 μl of plasma from each macaque and protein A Sepharose beads. The immunoprecipitates bound to the beads were washed three times in 1× RIPA, resuspended in 75 μl of 2× sample reducing buffer, and boiled for 5 min. Proteins were separated on a 10% SDS-PAGE gel and visualized by autoradiography. Controls included pooled prebleed plasma from macaques (negative control) and plasma from macaques that had been previously inoculated with a non-pathogenic SHIV ($SHIV_{TM,}$ positive control).

Acknowledgments

The work reported here is supported by grants NIH grants AI64019 and AI51981 to E.B.S. The pcDNA3.1(+)-rhesus A3G-HA and pcDNA3.1(+)-rhesus A3F-V5 were kindly provided by Dr. Nathaniel Landau (New York University School of Medicine, New York, New York). The TZM-bl cells were obtained through the NIH AIDS Research and Reference Reagent Program, Division of AIDS, NIAID, NIH and were from Drs. John C. Kappes and Xiaoyun Wu and Transzyme, Inc. We thank members of the KUMC Biotechnology Support Facility for their assistance with the sequence analysis and oligonucleotide synthesis.

References

Baba, T.W., Jeong, Y.S., Pennick, D., Bronson, R., Greene, M.F., Ruprecht, R.M., 1995. Pathogenicity of live, attenuated SIV after mucosal infection of neonatal macaques. Science 267, 1820–1825.

Baba, T.W., Liska, V., Khimani, A.H., Ray, N.B., Dailey, P.J., Penninck, D., Bronson, R., Greene, M.F., McClure, H.M., Martin, L.N., Ruprecht, R.M., 1999. Live attenuated, multiply deleted simian immunodeficiency virus causes AIDS in infant and adult macaques. Nat. Med. 5, 194–203.

Borman, A.M., Quillent, C., Charneau, P., Dauguet, C., Clavel, F., 1995. Human immunodeficiency virus type 1 Vif-mutant particles from restrictive cells: role of Vif in correct particle assembly and infectivity. J. Virol. 69, 2058–2067.

Blanc, D., Patience, C., Schulz, T.F., Weiss, R., Spire, B., 1993. Transcomplementation of VIF-HIV-1 mutants in CEM cells suggests that VIF affects late steps of the viral life cycle. Virology 193, 186–192.

Chen, G., He, Z., Wang, T., Xu, R., Yu, X.F., 2009. A patch of positively charged amino acids surrounding the human immunodeficiency virus type 1 Vif SLVx4Yx9Y motif influences its interaction with APOBEC3G. J. Virol. 83, 8674–8682.

Dang, Y., Wang, X., Zhou, T., York, I.A., Zheng, Y.H., 2009. Identification of a novel WxSLVK motif in the N terminus of human immunodeficiency virus and simian immunodeficiency virus Vif that is critical for APOBEC3G and APOBEC3F neutralization. J. Virol. 83, 8544–8552.

Dang, Y., Wang, X., Esselman, W.J., Zheng, Y.-H., 2006. Identification of APOBEC3DE as another antiretroviral factor from the human APOBEC family. J. Virol. 80, 10522–10533.

Dang, Y., Siew, L.M., Wang, X., Han, Y., Lampen, R., Zheng, Y.H., 2008. Human cytidine deaminase APOBEC3H restricts HIV-1 replication. J. Biol. Chem. 283, 11606–11614.

Derdeyn, C.A., Decker, J.M., Sfakianos, J.N., Wu, X., O'Brien, W.A., Ratner, L., Kappes, J.C., Shaw, G.M., Hunter, E., 2000. Sensitivity of human immunodeficiency virus type 1 to the fusion inhibitor T-20 is modulated by coreceptor specificity defined by the V3 loop of gp120. J. Virol. 74, 8358–8367.

Desrosiers, R.C., Lifson, J.D., Gibbs, J.S., Czajak, S.C., Howe, A.Y., Arthur, L.O., Johnson, R.P., 1998. Identification of highly attenuated mutants of simian immunodeficiency virus. J. Virol. 72, 1431–1437.

Doehle, B.P., Schafer, A., Cullen, B.R., 2005. Human APOBEC3B is a potent inhibitor of HIV-1 infectivity and is resistant to Vif. Virology 339, 281–288.

Fan, L., Peden, K., 1992. Cell-free transmission of Vif mutants of HIV-1. Virology 190, 19–29.

Gabuzda, D.H., Lawrence, K., Langhoff, E., Terwilliger, E., Dorfman, T., Haseltine, W.A., Sodroski, J., 1992. Role of vif in replication of human immunodeficiency virus type 1 in CD4+ T lymphocytes. J. Virol. 66, 6489–6495.

Harris, R.S., Bishop, K.N., Sheehy, A.M., Craig, H.M., Petersen-Mahrt, S.K., Watt, I.N., Neuberger, M.S., Malim, M.H., 2003. DNA deamination mediates innate immunity to retroviral infection. Cell 113, 803–809.

Hill, M.S., Mulcahy, E.R., Gomez, L.M., Miller, J.M., Berman, N.E., Stephens, E.B., 2006. APOBEC3G expression is restricted to neurons in the brains of macaques. AIDS Res. Hum. Retroviruses 22, 541–550.

Hill, M.S., Ruiz, A., Gomez, L.M., Miller, J.M., Berman, N.E., Stephens, E.B., 2007. APOBEC3G expression is restricted to epithelial cells of the proximal convoluted tubules and is not expressed in the glomeruli of macaques. J. Histochem. Cytochem. 55, 63–70.

Hill, M.S., Ruiz, A., Pacyniak, E., Pinson, D.M., Culley, N., Yen, B., Wong, S.W., Stephens, E.B., 2008. Modulation of the severe CD4+ T-cell los caused by a pathogenic simian-human immunodeficiency virus by replacement of the subtype B vpu from a subtype C HIV-1 clinical isolate. Virology 371 (1), 86–97.

Hofmann-Lehmann, R., Swenerton, R.K., Liska, V., Leutenegger, C.M., Lutz, H., McClure, H.M., Ruprecht, R.M., 2000. Sensitive and robust one-tube real-time reverse transcriptase-polymerase chain reaction to quantify SIV RNA load: comparison of one- versus two-enzyme systems. AIDS Res. Hum. Retroviruses 16, 1247–1257.

Hout, D.R., Gomez, M.L., Pacyniak, E., Gomez, L.M., Inbody, S.H., Mulcahy, E.R., Culley, N., Pinson, D.M., Powers, M.F., Wong, S.W., Stephens, E.B., 2005. Scrambling of the amino acids within the transmembrane domain of Vpu results in a simian-human immunodeficiency virus ($SHIV_{TM}$) that is less pathogenic for pig-tailed macaques. Virology 339, 56–69.

Hout, D.R., Gomez, M.L., Pacyniak, E., Gomez, L.M., Fegley, B., Mulcahy, E.R., Hill, M.S., Culley, N., Pinson, D.M., Nothnick, W., Powers, M.F., Wong, S.W., Stephens, E.B., 2006. Substitution of the transmembrane domain of Vpu in simian-human immunodeficiency virus ($SHIV_{KU1bMC33}$) with that of M2 of influenza A results in a virus that is sensitive to inhibitors of the M2 ion channel and is pathogenic for pig-tailed macaques. Virology 344, 541–559.

Jarmuz, A., Chester, A., Bayliss, J., Gisbourne, J., Dunham, I., Scott, J., Navaratnam, N., 2002. An anthropoid-specific locus of orphan C to U RNA-editing enzymes on chromosome 22. Genomics 79, 285–296.

Joag, S.V., Li, Z., Wang, C., Jia, F., Foresman, L., Adany, I., Pinson, D.M., Stephens, E.B., Narayan, O., 1998. Chimeric SHIV that causes CD4+ T cell loss and AIDS in rhesus macaques. J. Med. Primatol. 27 (2–3), 59–64.

Kim, E.Y., Busch, M., Abel, K., Fritts, L., Bustamante, P., Stanton, J., Lu, D., Wu, S., Glowczwskie, J., Rourke, T., Bogdan, D., Piatak Jr, M., Lifson, J.D., Desrosiers, R.C., Wolinsky, S., Miller, C.J., 2005. Retroviral recombination in vivo: viral replication patterns and genetic structure of simian immunodeficiency virus (SIV) populations in rhesus macaques after simultaneous or sequential intravaginal inoculation with SIVmac239Deltavpx/Deltavpr and SIVmac239Deltanef. J. Virol. 79, 4886–4895.

Koff, W.C., Johnson, P.R., Watkins, D.I., Burton, D.R., Lifson, J.D., Hasenkrug, K.J., McDermott, A.B., Schultz, A., Zamb, T.J., Boyle, R., Desrosiers, R.C., 2006. HIV vaccine design: insights from live attenuated SIV vaccines. Nat. Immunol. 7, 19–23.

Luo, K., Xiao, Z., Ehrlich, E., Yu, Y., Liu, B., Zheng, S., Yu, X.F., 2005. Primate lentiviral virion infectivity factors are substrate receptors that assemble with cullin 5-E3 ligase through a HCCH motif to suppress APOBEC3G. Proc. Natl Acad. Sci. USA 102, 11444–11449.

Mangeat, B., Turelli, P., Caron, G., Friedli, M., Perrin, L., Trono, D., 2003. Broad antiretroviral defence by human APOBEC3G through lethal editing of nascent reverse transcripts. Nature 424, 99–103.

Marcario, J.K., Riazi, M., Adany, R.I., Kenjale, H., Fleming, K., Marquis, J., Nemon, O., Mayo, S., Yankee, T., Narayan, O., Cheney, P.D., 2008. Effect of morphine on the neuropathogenesis of SIVmac infection in Indian rhesus macaques. J. Neuroimmune Pharmacol. 3 (12), 12–25.

Mariani, R., Chen, D., Schrofelbauer, B., Navarro, F., Konig, R., Bollman, B., Munk, C., Nymark-McMahon, H., Landau, N.R., 2003. Species-specific exclusion of APOBEC3G from HIV-1 virions by Vif. Cell 114, 21–31.

Mehle, A., Goncalves, J., Santa-Marta, M., McPike, M., Gabuzda, D., 2004a. Phosphorylation of a novel SOCS-box and upstream cysteines. Genes Dev. 18, 2867–2872.

Mehle, A., Strack, B., Ancuta, P., Zhang, C., McPike, M., Gabuzda, D., 2004b. Vif overcomes the innate antiviral activity of APOBEC3G by promoting its degradation in the ubiquitin–proteasome pathway. J. Biol. Chem. 279, 7792–7798.

Mehle, A., Thomas, E.R., Rajendran, K.S., Gabuzda, D., 2006. A zinc-binding region in Vif binds Cul5 and determines cullin selection. J. Biol. Chem. 281, 17259–17265.

Mehle, A., Wilson, H., Zhang, C., Brazier, A.J., McPike, M., Pery, E., Gabuzda, D., 2007. Identification of an APOBEC3G binding site in human immunodeficiency virus type1 Vif and inhibitors of Vif-APOBEC3G binding. J. Virol. 81, 13235–13241.

Pery, E., Rajendran, K.S., Brazier, A.J., Gabuzda, D., 2009. Regulation of APOBEC3 proteins by a novel YXXL motif in human immunodeficiency virus type 1 Vif and simian immunodeficiency virus SIVagm Vif.

Russell, R.A., Pathak, V.K., 2007. Identification of two distinct human immunodeficiency virus type 1 Vif determinants critical for interactions with human APOBEC3G and APOBEC3F. J. Virol. 81, 8201–8210.

Sakai, H., Shibata, R., Sakuragi, J., Sakuragi, S., Kawamura, M., Adachi, A., 1993. Cell-dependent requirement of human immunodeficiency virus type 1 Vif protein for maturation of virus particles. J. Virol. 67, 1663–1666.

Schmitt, K., Hill, M.S., Ruiz, A., Culley, N., Pinson, D.M., Wong, S.W., Stephens, E.B., 2009. Mutations in the highly conserved SLQYLA motif of Vif in a simian-human immunodeficiency virus result in a less pathogenic virus and are associated with G-to-A mutations in the viral genome. Virology 383, 362–372.

Sheehy, A.M., Gaddis, N.C., Malim, M.H., 2003. The antiretroviral enzyme APOBEC3G is degraded by the proteasome in response to HIV-1 Vif. Nat. Med. 9, 1404–1407.

Shindo, K., Takaori-Kondo, A., Kobayashi, M., Abudu, A., Fukunaga, K., Uchiyama, T., 2003. The enzymatic activity of CEM15/Apobec-3G is essential for the regulation of the infectivity of HIV-1 virion but not a sole determinant of its antiviral activity. J. Biol. Chem. 278, 44412–44416.

Singh, D.K., Griffin, D.M., Pacyniak, E., Jackson, M., Werle, M.J., Wisdom, B., Sun, F., Hout, D.R., Pinson, D.M., Gunderson, R.S., Powers, M.F., Wong, S.W., Stephens, E.B., 2003. The presence of the casein kinase II phosphorylation sites of Vpu enhances the $CD4^+$ T cell loss caused by the simian-human immunodeficiency virus $SHIV_{KU-1bMC33}$ in pig-tailed macaques. Virology 313, 435–451.

Sparger, E.E., Dubie, R.A., Shacklett, B.L., Cole, K.S., Chang, W.L., Luciw, P.A., 2008. Vaccination of rhesus macaques with a vif-deleted simian human immunodeficiency virus proviral DNA vaccine. Virology 374, 261–272.

Stephens, E.B., McCormick, C., Pacyniak, E., Griffin, D., Pinson, D.M., Sun, F., Nothnick, W., Wong, S.W., Gunderson, R., Berman, N.E., Singh, D.K., 2002. Deletion of the *vpu* sequences prior to the *env* in a simian-human immunodeficiency virus results in enhanced Env precursor synthesis but is less pathogenic for pig-tailed macaques. Virology 293, 252–261.

Stopak, K., de Noronha, C., Yonemoto, W., Greene, W.C., 2003. HIV-1 Vif blocks the antiviral activity of APOBEC3G by impairing both its translation and intracellular stability. Mol. Cell. 12, 591–601.

von Schwedler, U., Song, J., Aiken, C., Trono, D., 1993. Vif is crucial for human immunodeficiency virus type 1 proviral DNA synthesis in infected cells. J. Virol. 67, 4945–4955.

Virgen, C.A., Hatziioannou, T., 2007. Antiretroviral activity and Vif sensitivity of rhesus macaque APOBEC3 proteins. J. Virol. 81, 13932–13937.

Wei, X., Decker, J.M., Liu, H., Zhang, Z., Arani, R.B., Kilby, J.M., Saag, M.S., Wu, X., Shaw, G.M., Kappes, J.C., 2000. Emergence of resistant human immunodeficiency virus type 1 in patients receiving fusion inhibitor (T-20) monotherapy. Antimicrob. Agents Chemother. 46, 1896–1905.

Wiegand, H.L., Doehle, B.P., Bogerd, H.P., Cullen, B.R., 2004. A second human antiretroviral factor, APOBEC3F, is suppressed by the HIV-1 and HIV-2 Vif proteins. EMBO J. 23, 2451–2488.

Xiao, Z., Xiong, Y., Zhang, W., Tan, L., Ehrlich, E., Guo, D., Yu, X.F., 2007. Characterization of a novel Cullin5 binding domain in HIV-1 Vif. J. Mol. Biol. 373, 541–550.

Yang, Y., Guo, F., Cen, S., Kleiman, L., 2007. Inhibition of initiation of reverse transcription in HIV-1 by human APOBEC3F. Virology 365, 92–100.
Yu, Q., Konig, R., Pillai, S., Chiles, K., Kearney, M., Palmer, S., Richman, D., Coffin, J.M., Landau, N.R., 2004a. Single-strand specificity of APOBEC3G accounts for minus-strand deamination of the HIV genome. Nat. Struct. Mol. Biol. 11, 435–442.
Yu, Q., Chen, D., Konig, R., Mariani, R., Unutmaz, D., Landau, N.R., 2004b. APOBEC3B and APOBEC3C are potent inhibitors of simian immunodeficiency virus replication. J. Biol. Chem. 279, 53379–53386.
Yu, X., Yu, Y., Liu, B., Luo, K., Kong, W., Mao, P., Yu, X.F., 2003. Induction of APOBEC3G ubiquitination and degradation by an HIV-1 Vif-Cul5-SCF complex. Science 302, 1056–1060.
Yu, Y., Xiao, Z., Ehrlich, E.S., Yu, X., Yu, X.F., 2004c. Selective assembly of HIV-1 Vif-Cul5-ElonginB-ElonginC E3 ubiquitin ligase complex through a novel SOCS box and upstream cysteines. Genes Dev. 18, 2867–2872.
Zennou, V., Bieniasz, P.D., 2006. Comparative analysis of the antiretroviral activity of APOBEC3G and APOBEC3F from primates. Virology 349, 31–40.
Zhang, H., Yang, B., Pomerantz, R.J., Zhang, C., Arunachalam, S.C., Gao, L., 2003. The cytidine deaminase CEM15 induces hypermutation in newly synthesized HIV-1 DNA. Nature 424, 94–98.
Zheng, Y.H., Irwin, D., Kurosu, T., Tokunaga, K., Sata, T., Peterlin, B.M., 2004. Human APOBEC3F is another host factor that blocks human immunodeficiency virus type 1 replication. J. Virol. 78, 6072–6076.